NAVY DEPARTMENT

THE DAVID W. TAYLOR MODEL BASIN

WASHINGTON 7, D.C.

HYDROSTATIC PRESSURE TESTS ON THIN RECTANGULAR DIAPHRAGMS 84 INCHES BY 54 INCHES

By

John W. Day

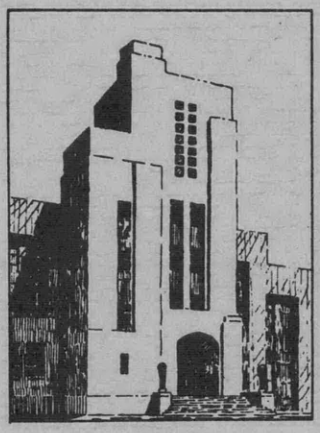

September 1951

Revised Edition

Report 636

NS 724-008

INITIAL DISTRIBUTION

Copies

8 Chief, BuShips, Project Records (Code 324), for distribution:
- 5 Project Records
- 1 Technical Assistant (Code 106)
- 2 Underwater Explosion Research (Code 423)

2 Commander, Norfolk Naval Shipyard, Portsmouth, Va., Attn: Underwater Explosions Research Division, Code 290

TABLE OF CONTENTS

HYDROSTATIC PRESSURE TESTS ON THIN RECTANGULAR DIAPHRAGMS 84 INCHES BY 54 INCHES

by

John W. Day

ABSTRACT

Hydrostatic-pressure tests of thin, clamped, rectangular diaphragms 84 inches by 54 inches were conducted in connection with the general underwater-explosion research program. Data such as profiles of deflected diaphragms, curves of center deflection against pressure, thickness, horizontal displacement, strain, volume of displacement of deflected diaphragms, and energy absorbed were obtained for each of the four diaphragms tested. The results of these tests were compared with results of similar tests on small diaphragms and with a theory for rectangular diaphragms under hydrostatic pressure previously developed at the Taylor Model Basin.

The energy absorbed by the large diaphragms when compared with the energy absorbed by the small diaphragms was less than had been expected.

INTRODUCTION

The Bureau of Ships requested the David Taylor Model Basin to conduct hydrostatic-pressure tests on thin, rectangular, clamped diaphragms 84 inches by 54 inches, as one of many projects of the general underwater-explosion research program.[1,2] The technique for testing these diaphragms was developed during a series of similar tests[3] on thin rectangular diaphragms 21 inches by 13 1/2 inches.

The tests on rectangular diaphragms described in this report are a direct continuation of the work reported in Reference 3 and are related to initial tests on 20-inch circular diaphragms reported in Reference 4. The results of the hydrostatic tests on both circular and rectangular diaphragms supplement the results of explosion tests on similar diaphragms at the Norfolk Naval Shipyard and offer a basis for analysis of the explosion work.

Four medium-steel diaphragms were tested, two 1/8-inch thick and two 3/16-inch thick. For each of the diaphragms data such as profiles of the deflected diaphragms, curves of center deflection against pressure, thickness,

---

[1]References are listed on page 39.

horizontal displacement, volume of displacement of the deflected diaphragm, and energy absorbed were measured or computed.

In this report the technique for testing large rectangular diaphragms is described, the results of hydrostatic-pressure tests are presented, and the experimental results are compared with the theory of Reference 5.

TEST SETUP AND PROCEDURE

A frame was designed for testing, under hydrostatic pressure, rectangular diaphragms with a free area of 7 feet by 4 1/2 feet. The principal components of the assembly were two clamping frames and a heavy plate called a compression plate (Figure 1).

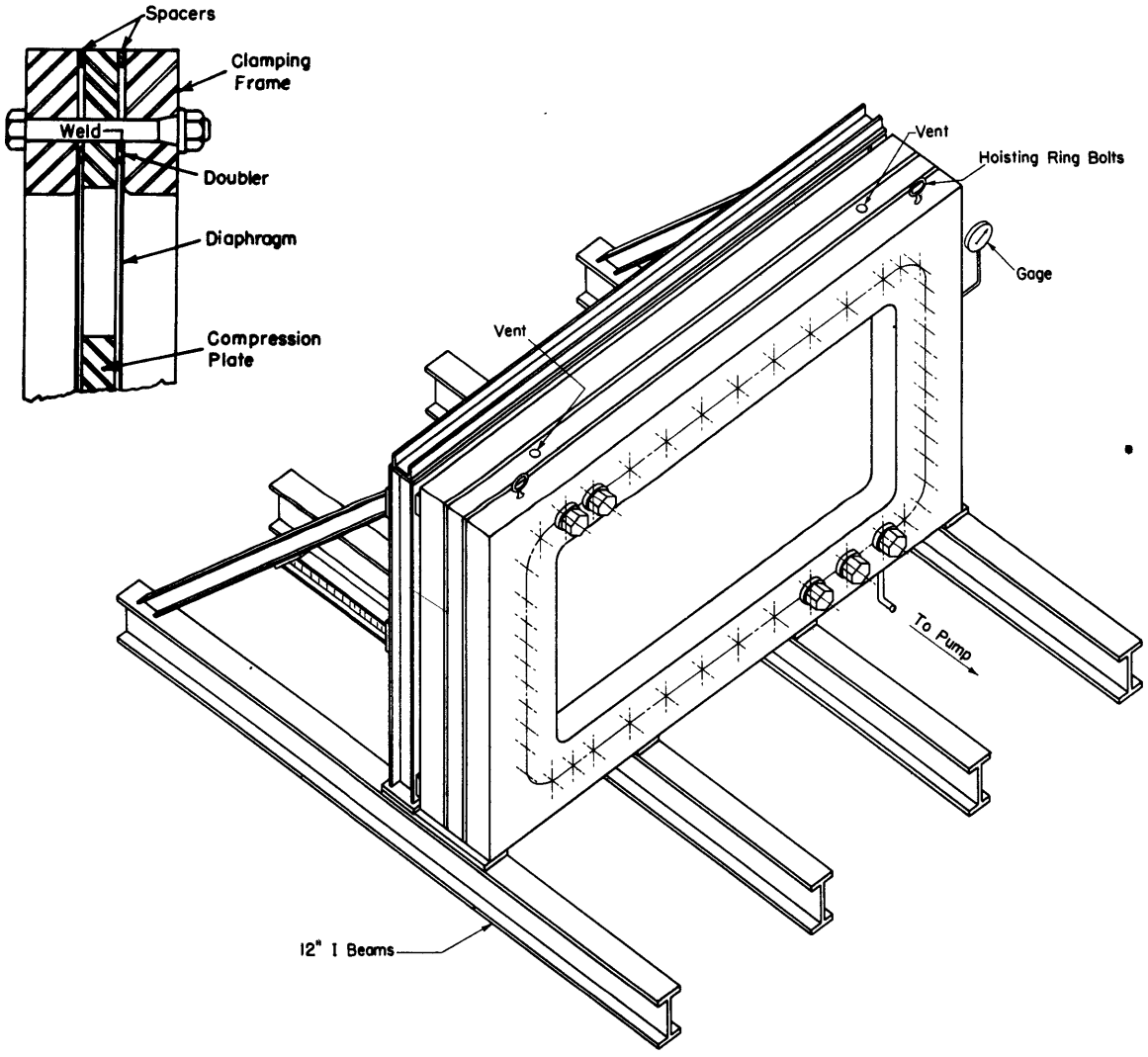

Figure 1 - Isometric and Sectional Sketch of Test Assembly

One clamping frame was permanently mounted on the support frame as shown in Figure 2. Before the diaphragms to be tested were welded to the compression plate, a doubler strip 1 inch wide by 5/8 inch thick was welded around the edge of each diaphragm on the pressure side. This doubler allowed a heavier weld to the compression plate. The diaphragm and doubler were then welded to the compression plate (Figure 3). Spacer straps, as thick as the doubler and diaphragm combined, were screwed to the edge of the compression plate to provide even bearing for the clamping frames.

The simplified grid system shown in Figure 4a was used on the first pair of diaphragms tested, as the measuring rig was not yet available. A grid system of 8-inch squares was laid out on the other pair of diaphragms as shown in detail in Figure 4b. Optical-black lacquer was used as a base for scribing grid lines on the diaphragms. Grid-line intersections were marked by light punch marks to facilitate locating the pointer on the measuring rig.

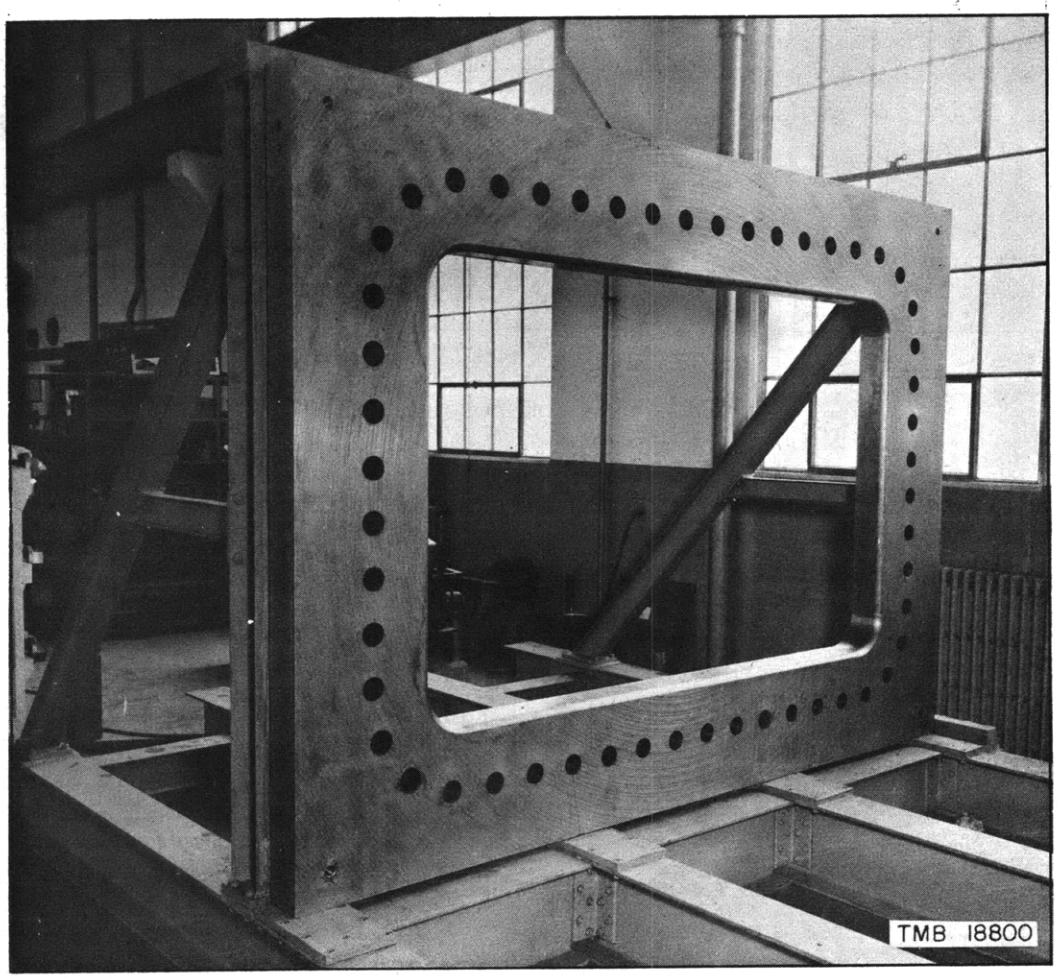

Figure 2 - Clamping Frame Mounted in Support Frame

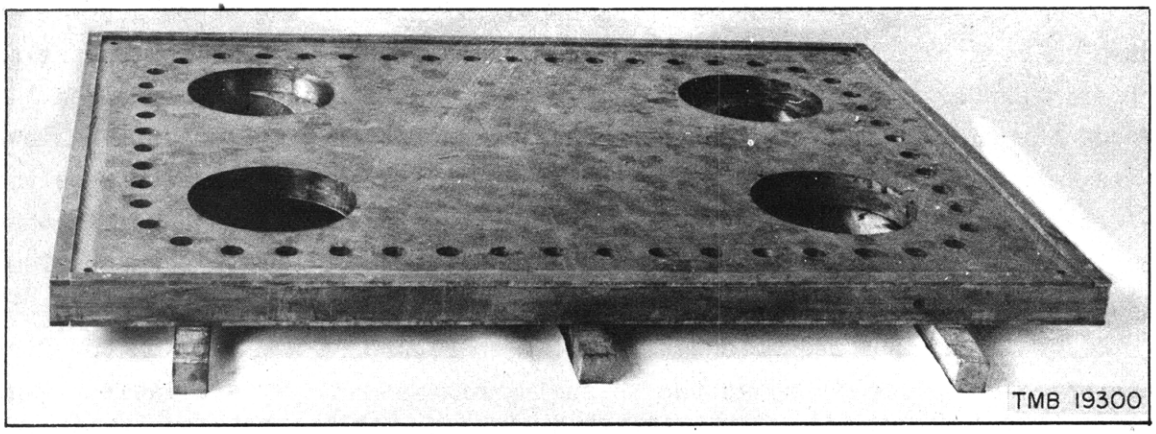

Figure 3a - Compression Plate with Spacers Ready for Welding on Diaphragms

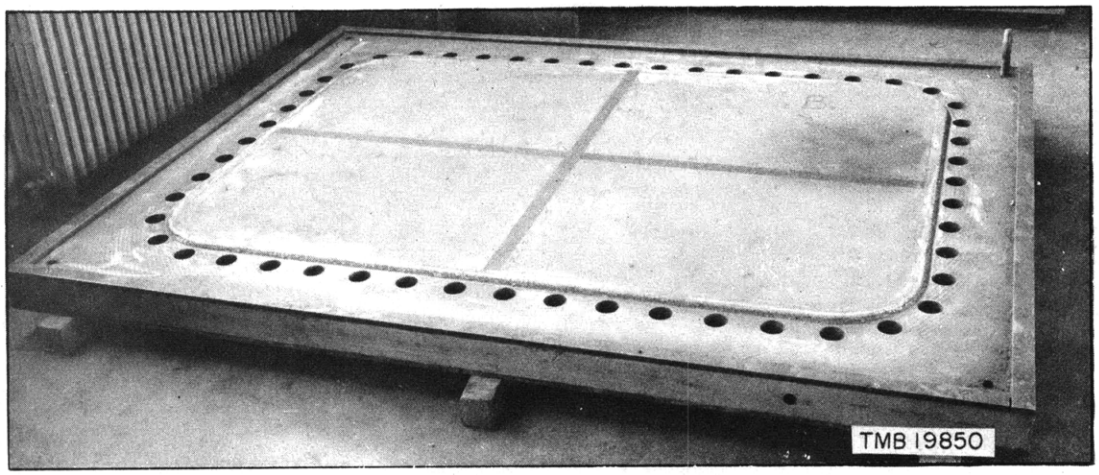

Figure 3b - Compression Plate with Diaphragm Welded in Place

Figure 3 - Compression Plate

After the diaphragms had been welded to the compression plate and marked with grid lines, the plate was assembled with the clamping frames. The compression plate and clamping frame were placed in the permanent part of the assembly shown in Figure 2 in the order named. These heavy units were then aligned and bolted together. The diaphragm assembly was then filled with water by means of two vent holes in the top edge of the compression plate. (One hole is used for filling while the other hole vents the air.) Care was exercised to expel all air from the diaphragm and hydraulic system before testing was started.

Tracks for the measuring rig were bolted to the top and bottom of both clamping frames as shown in Figure 5. The traveling beam of the measuring rig moved along the upper track; the lower track was only a guide track. When readings were being taken, the ends of the traveling beam were positioned

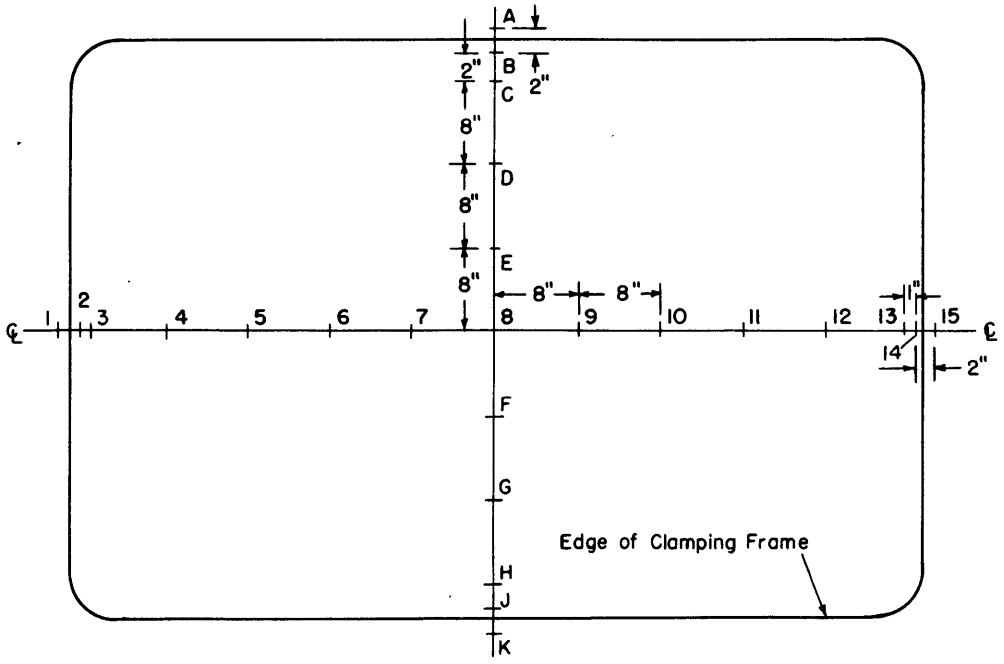

Figure 4a - Diaphragms 1A and 1B

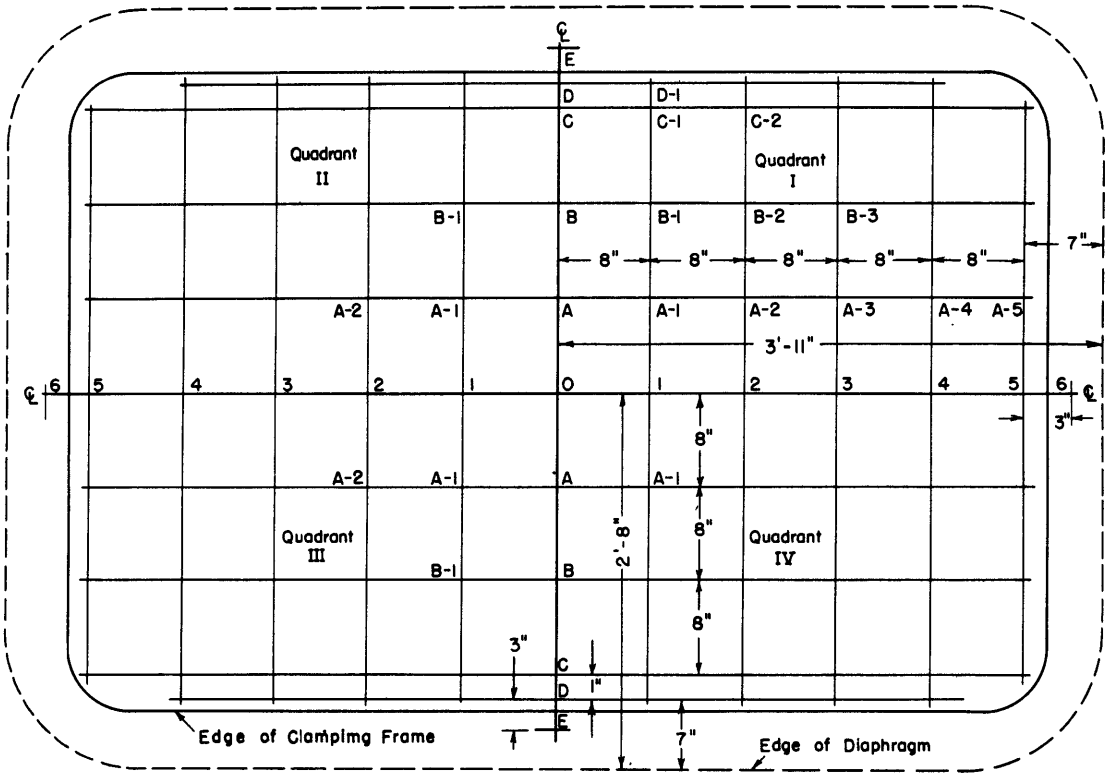

Figure 4b - Diaphragms 2A and 2B

Figure 4 - Grid Layouts for Rectangular Diaphragms

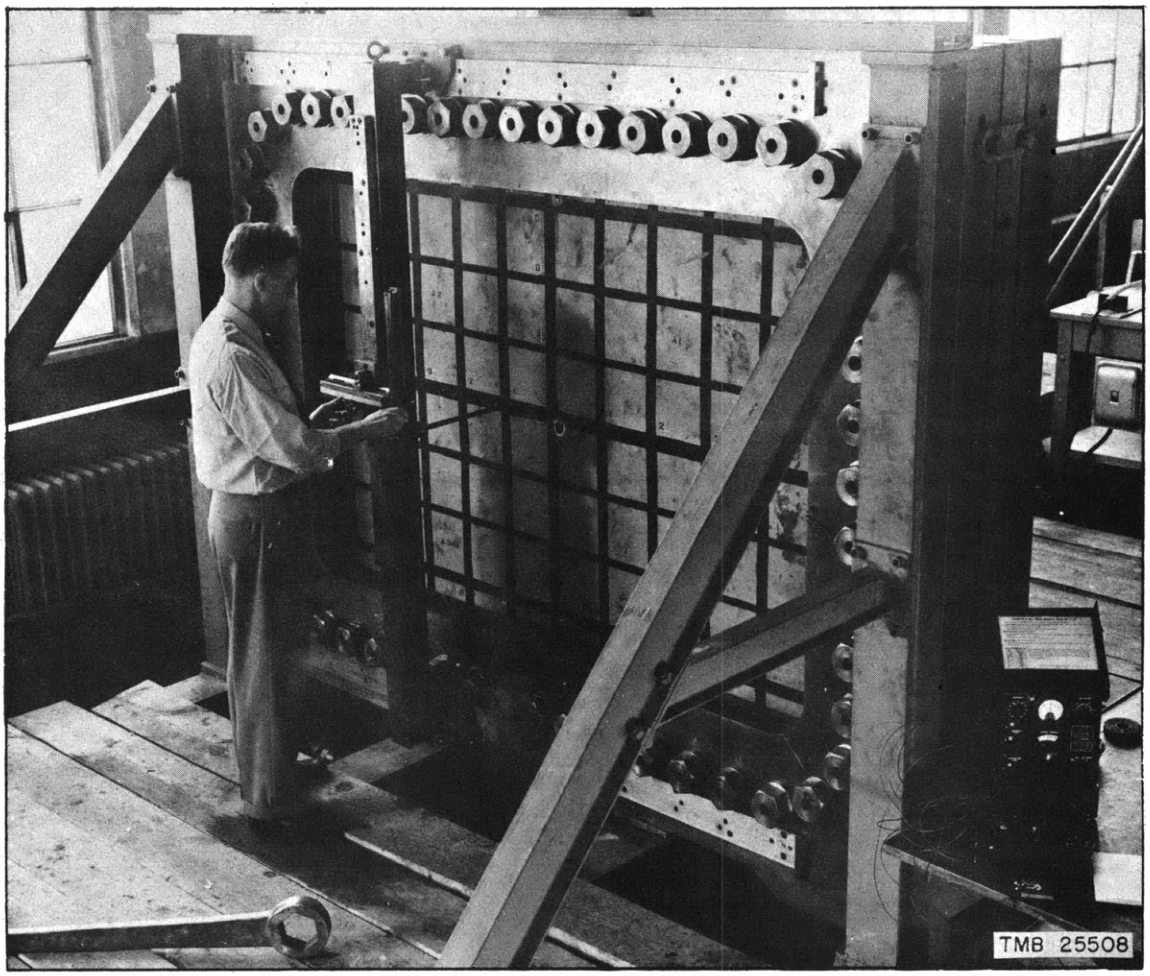

Figure 5 - General View of Diaphragm Test Assembly with Measuring Rig in Operating Position

by tapered pins inserted in matching holes in the beam-support pad and the track; two socket-head screws securely fixed each end of the pad to the track. A similar arrangement was used for securing the measuring carriage to the beam. Figure 6 shows a close-up view of the carriage with the tapered positioning pin and socket-head screws clearly shown. Tee wrenches were permanently welded to the socket-head screws to facilitate operation of the measuring carriage. The measuring rig could be used on either diaphragm.

A pressure gage was mounted in a vent hole in the vertical edge of the compression plate so that the gage was at about mid-height of the diaphragm and gave a reading of the average pressure on the diaphragm. Pressure was applied by means of a hand pump with a capacity of 1500 to 6000 psi.

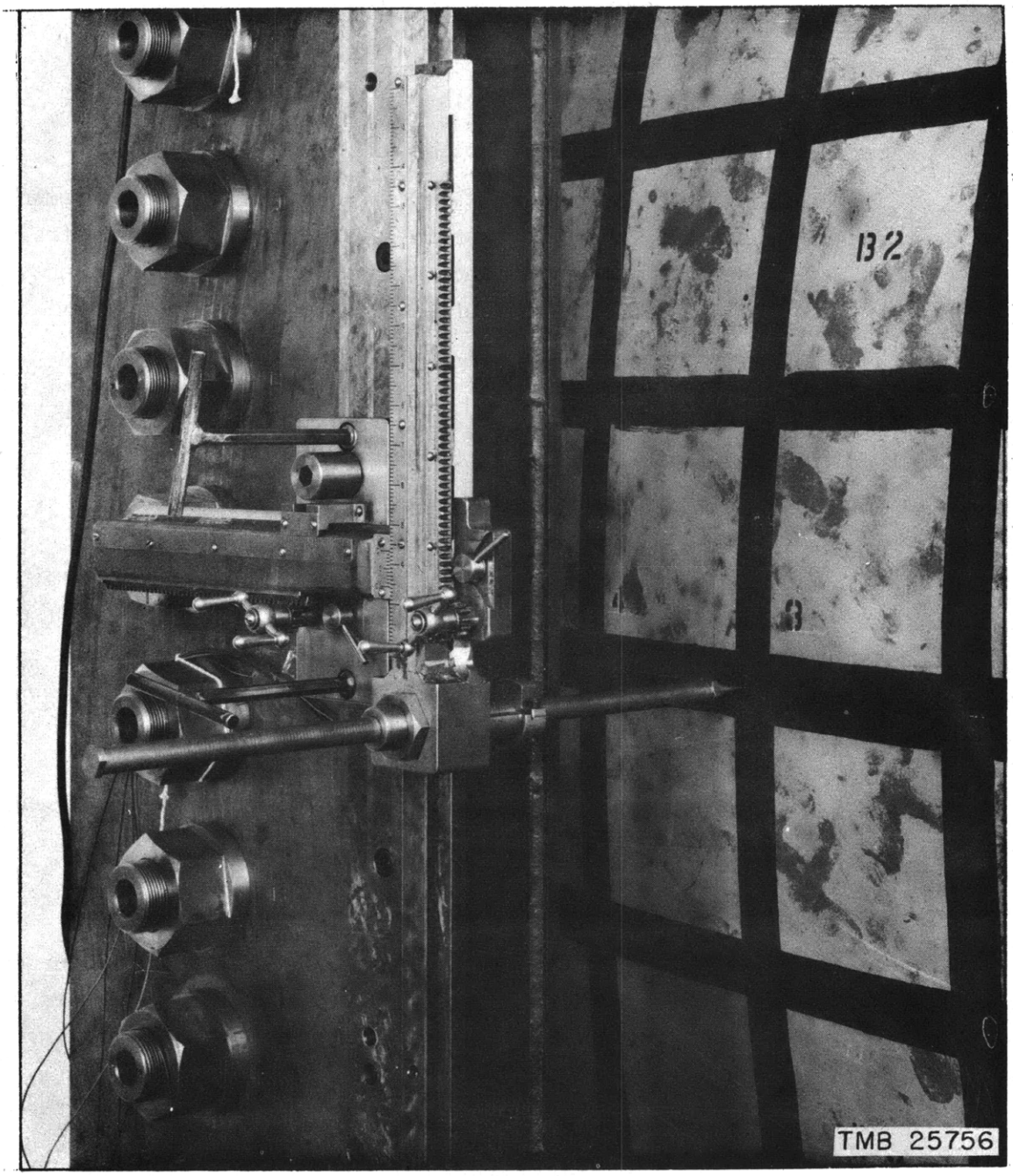

Figure 6 - Details of Rig for Measuring Displacements of Points on the Diaphragm

Displacements of each of the diaphragms were measured at each intersection of the grid lines before pressure was applied, after each increment of pressure, after relaxation of each pressure increment, and after rupture of one of the two diaphragms. These displacements were measured in three directions:

1. Parallel to the original plane of the diaphragm in a longitudinal direction.

2. Parallel to the original plane in a transverse direction.

3. Perpendicular to the original plane.

The strains in the diaphragms were computed from the displacements instead of being measured by the usual strain-gage method. Expected strains were of such magnitude that wire-resistance gages were not considered adequate.

The volumes displaced by the deflected diaphragms were determined by metering the pressure medium. The energy absorbed by each diaphragm for each pressure was computed from these data. Initial and final thicknesses of the four diaphragms were measured at each grid intersection to determine the amount each diaphragm was thinned during testing.

TEST RESULTS AND DISCUSSION

A summary of the measured and computed results of the hydrostatic tests is given in Tables 1 and 2. The more detailed results are presented in the following sections.

Figure 7 shows a diaphragm test assembly after the test had been completed and one clamping frame had been removed. The arrow indicates the location of the rupture in the diaphragm. This is a typical example of rupture in the region of high bending stress where the diaphragm is bent over the rounded edge of the clamping frame.

MEASUREMENTS OF DISPLACEMENTS

Displacements of points on the diaphragms were measured in three planes perpendicular to each other. These displacements were determined for each increment of pressure at each of the grid intersections. All measurements were made to an accuracy of 0.005 inch.

The deflections of points along the major and minor axes of the diaphragms are plotted for each increment of pressure in Figure 8. Pressure readings were taken after the diaphragm had been subjected to a given pressure long enough for a stable condition to develop through plastic readjustments in the metal. The pressure was then released, and readings were again taken. Hence the difference between any deflection curve for a given pressure and the subsequent deflection curve for atmospheric pressure represents the elastic deflection of the material.

TABLE 1

Physical Data on Rectangular Medium-Steel Diaphragms

Diaphragm	Original Thickness $h_\square$ inches	Final Center Deflection $Z_\square$ inches	Rupture Pressure p psi	Equivalent Radius* Thickness Ratio $a_\square/h_\square$	Location and Type of Failure
1A	0.125	9.47		305	
1B	0.125	9.71	226	305	Failed in mid-lower edge of diaphragm
2A	0.182	7.06	245	209	Failed in mid-top edge of diaphragm
2B	0.182	7.07		209	

*Equivalent radius is defined by the equation

$$\frac{1}{a_\square^2} = \frac{16}{45}\left(\frac{1}{a_1^2} + \frac{1}{a_2^2}\right)$$

TABLE 2

Summary of Results of Hydrostatic Tests on Unstiffened Rectangular Diaphragms

Diaphragm	Final Measured Volume cu. ft.	Computed* Volume cu. ft.	Computed Volume Variance percent	Total Energy Absorbed $W = \int p\, dV$ Test Data ft-lb	Approximate Total Energy** Absorbed ft-lb	Approximate Energy Variance percent	Energy Absorbed ft-lb/lb
1A	13.00	11.63	-10.5	193,000	217,000	12.5	1205
1B	13.30	11.88	-10.7	196,500	226,500	15.2	1230
2A	9.365	8.50	-9.24	141,500	153,300	8.32	608
2B	9.365	8.50	-9.24	141,500	153,300	8.32	608

*The computed volume is equivalent to $\frac{16}{9} a_1 a_2 Z_\square$

**The approximate total energy is expressed by the equation

$$W_\square = \frac{64}{45}\left(\frac{a_2}{a_1} + \frac{a_1}{a_2}\right) \sigma_\square h_\square Z_\square^2$$

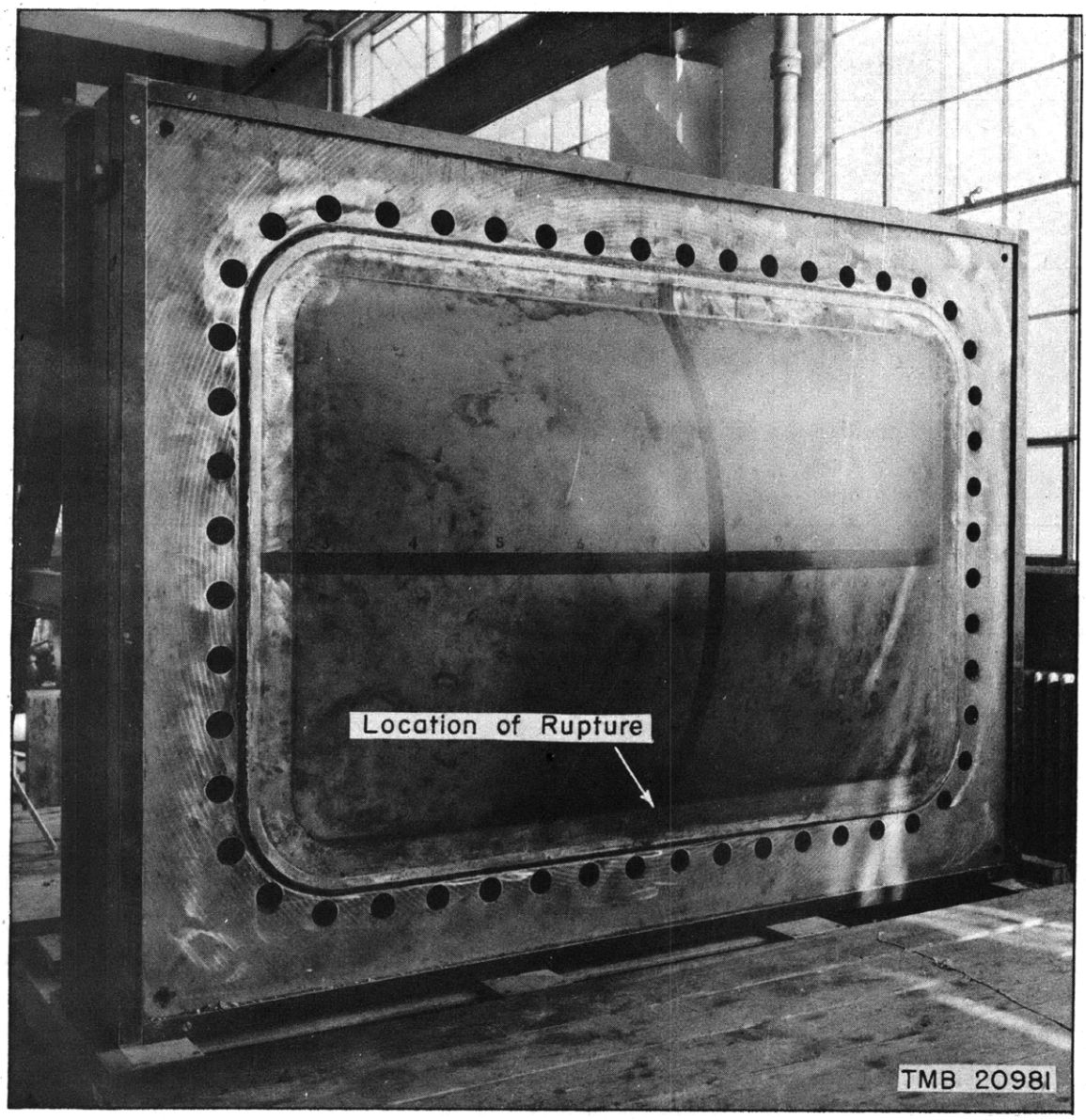

Figure 7 - Clamping Frame Removed to Show Diaphragm
After Testing and Location of Rupture

The center deflections of the four diaphragms tested are plotted against pressure in Figure 9. The points on the upper curves represent deflections of the centers of the diaphragms at the given pressures. The points on the curves of plastic deflection represent the deflections of the diaphragms after the pressure had been reduced to atmospheric pressure from the pressure of the corresponding point on the upper deflection curve.

The displacements parallel to the original plane of the diaphragm of points on the major and minor axes of the diaphragms are plotted in Figure 10. In the sketch the point P_o represents a grid station on the originally flat diaphragm. As the diaphragm deflects, the point P_o moves over the curved path to Point P. The quantities x in the case of the long axis and y in the case of the short axis represent the distance of the grid point from the center point of the originally flat diaphragm. The quantity u represents the horizontal displacement of the point after failure, with respect to the x or y axis.

MEASUREMENTS OF STRAIN

Figure 11 represents the grids marked on the test diaphragms in their initial flat state to form 8-inch squares. The values given represent the final average strains over the 8-inch base lengths in inches per inch. The strain values adjacent and normal to the long edges of the diaphragm are final average strains over 1-inch base lengths in inches per inch. Final strains were measured on the surface of the diaphragms and represent arc distances.

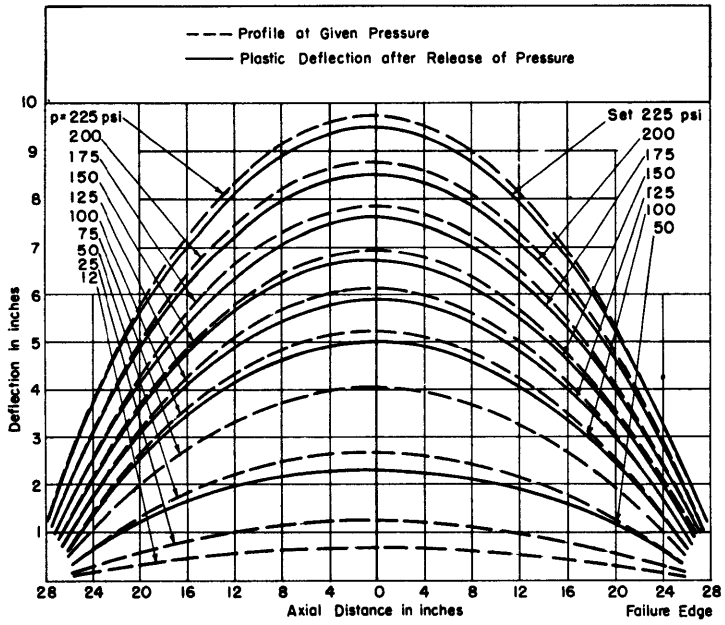

Figure 8a - Profiles of 1/8-Inch Medium-Steel Diaphragm 1B

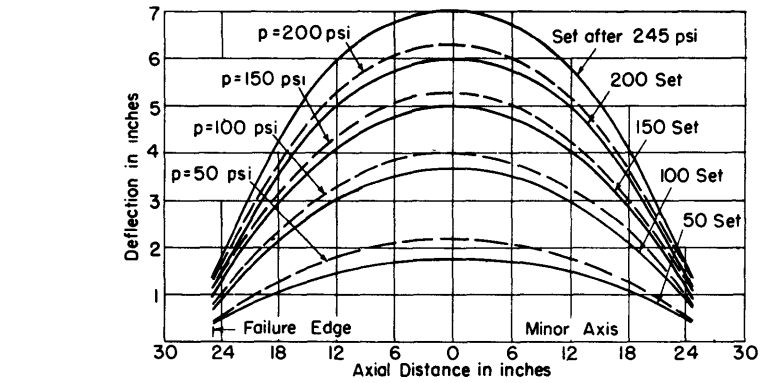

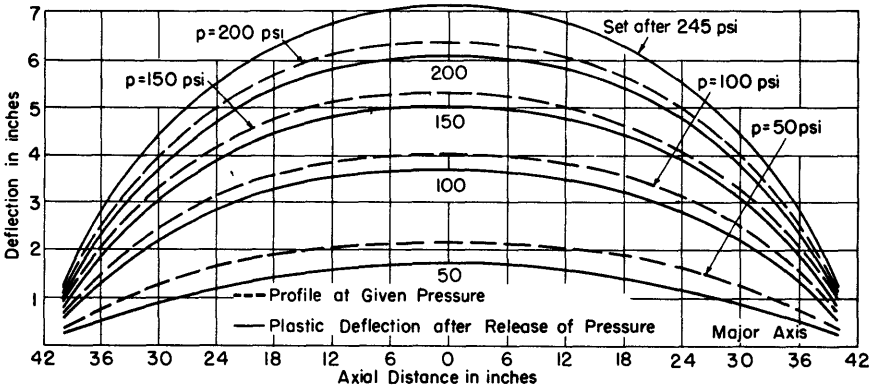

Figure 8b - Profiles of 3/16-Inch Medium-Steel Diaphragm 2A

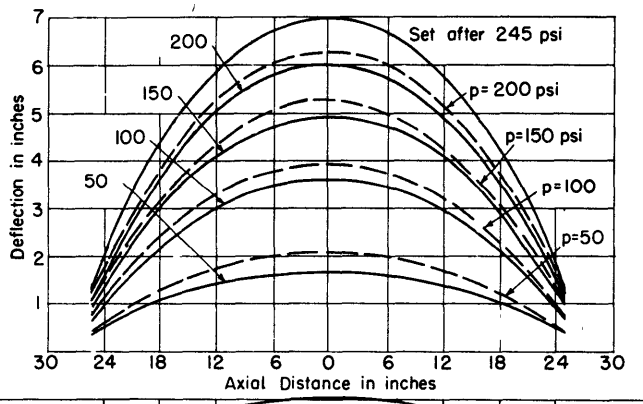

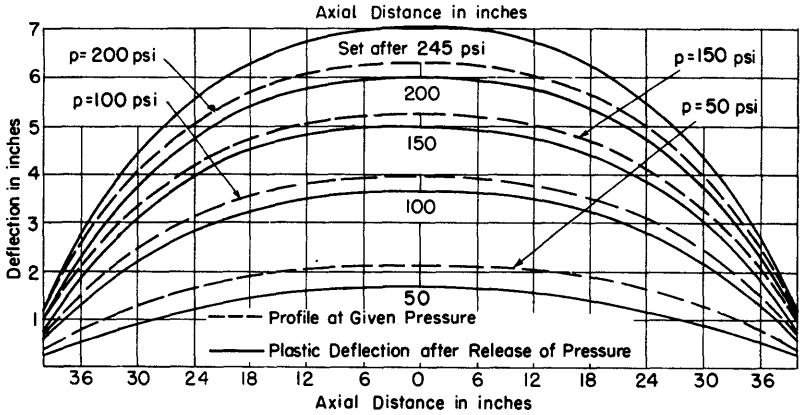

Figure 8c - Profiles of 3/16-Inch Medium-Steel Diaphragm 2B

Figure 8 - Profiles of Diaphragms at Various Pressures

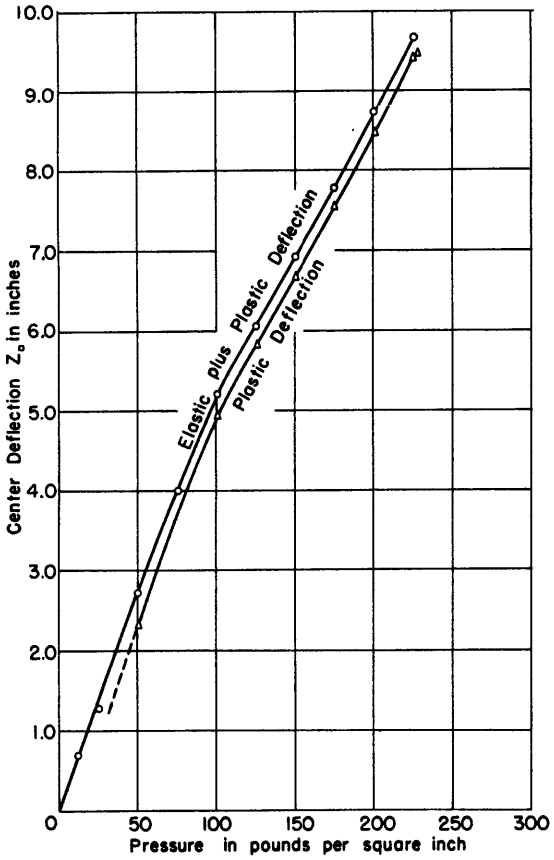

Figure 9a - Center Deflection of 1/8-Inch Medium-Steel Diaphragm 1A

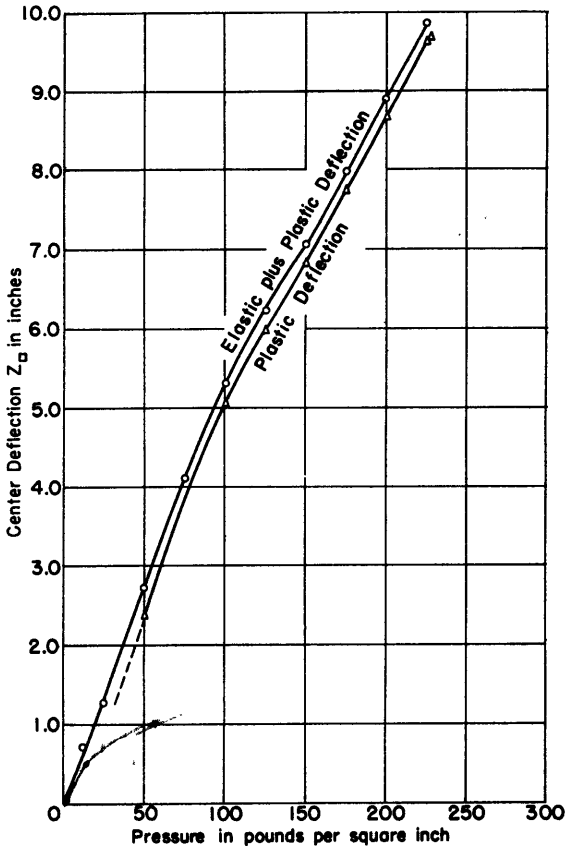

Figure 9b - Center Deflection of 1/8-Inch Medium-Steel Diaphragm 1B

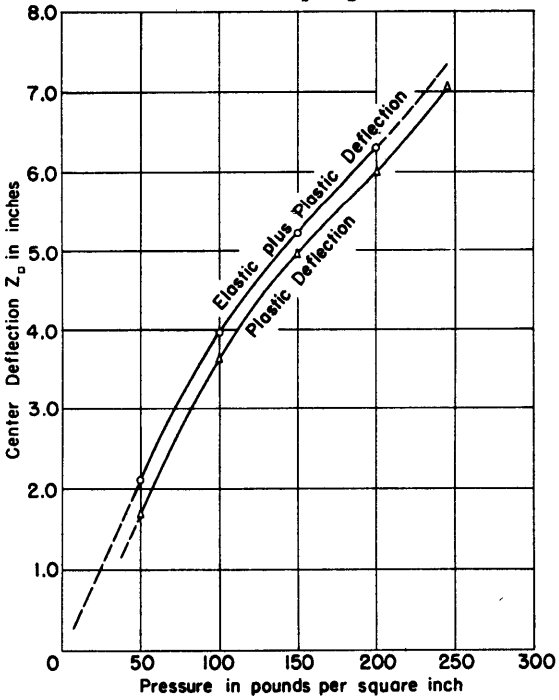

Figure 9c - Center Deflection of 3/16-Inch Medium-Steel Diaphragm 2A

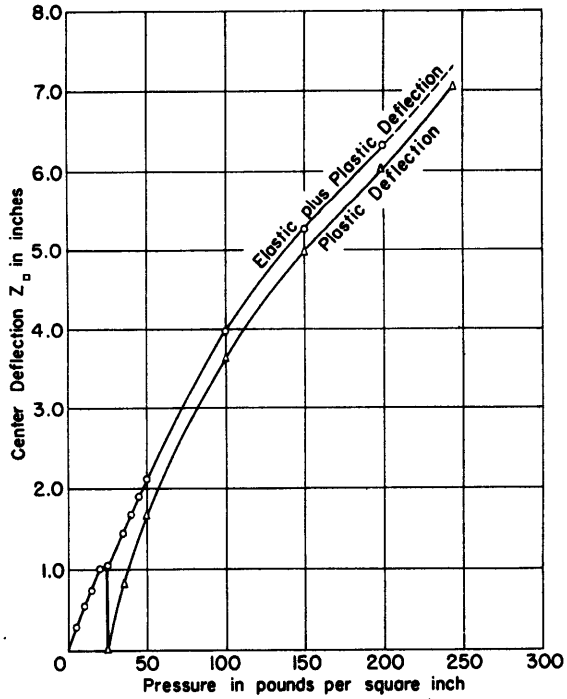

Figure 9d - Center Deflection of 3/I6-Inch Medium-Steel Diaphragm 2B

Figure 9 - Curves of Center Deflection vs Pressure

In Figures 12 through 15 strains on the longitudinal and transverse axes of the four diaphragms are plotted against center deflection. Each curve represents the strains at definite positions on the diaphragm as indicated in the sketch of the diaphragm showing the strain bases. The values of strain were computed from displacement data taken at specific points on the axes of the diaphragm. The strains are based on the change in chord lengths between adjacent grid intersections and are plotted at the midpoint of the initial base length. The cut-back or drop in the strain at the terminal point of many of the curves represents the elastic component of strain lost on relaxation of pressure on the diaphragm.

Figures 16 through 19 represent profiles of strain along the major and minor axes of the diaphragms. There is a strain-profile curve for each pressure increment taken during the test. The dotted curve in each figure represents the axial profile of plastic strain remaining in the diaphragm after it had been cut from the compression plate. The additional point on each end of this curve represents the plastic strain in the edge grid. These end points were inaccessible for measurement during the test.

MEASUREMENTS OF THICKNESS

The thickness of the diaphragms was measured at each grid intersection before and after testing by means of a dial-gage micrometer. These thicknesses are plotted in Figures 20 through 23.

VOLUME OF DISPLACEMENT BY DEFLECTION OF DIAPHRAGMS

The volume change for both diaphragms of a test assembly plotted against the average center deflection is represented in Figures 24 and 25. The volumes include the space between the initial planes of each diaphragm and the dished shape taken by the inside surfaces of the two diaphragms as a result of the application of hydrostatic pressure.

Measured volumes were determined by the metered fluid pumped into the diaphragms to deflect them a given amount at the center. Computed volumes are determined by use of the equation

$$V = \frac{16}{9} a_1 a_2 Z_\square$$

for any given center deflection selected. Discussion of this equation occurs in a later section.

Figure 26 contains curves of variance of computed volume from actual measured volume plotted against increments of test pressure.

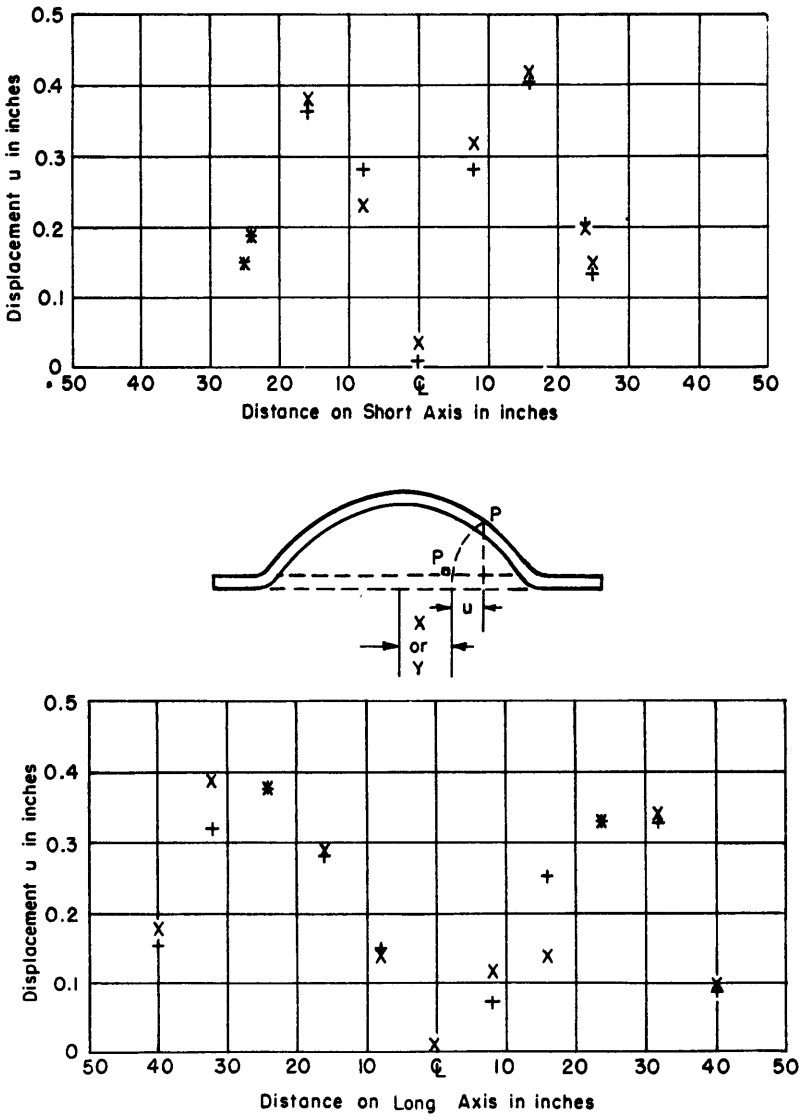

Figure 10 - Axial Displacements after Rupture of 3/16-Inch Diaphragms 2A and 2B

The graph symbols x represent points on Diaphragm 2A, the symbols + points on Diaphragm 2B.

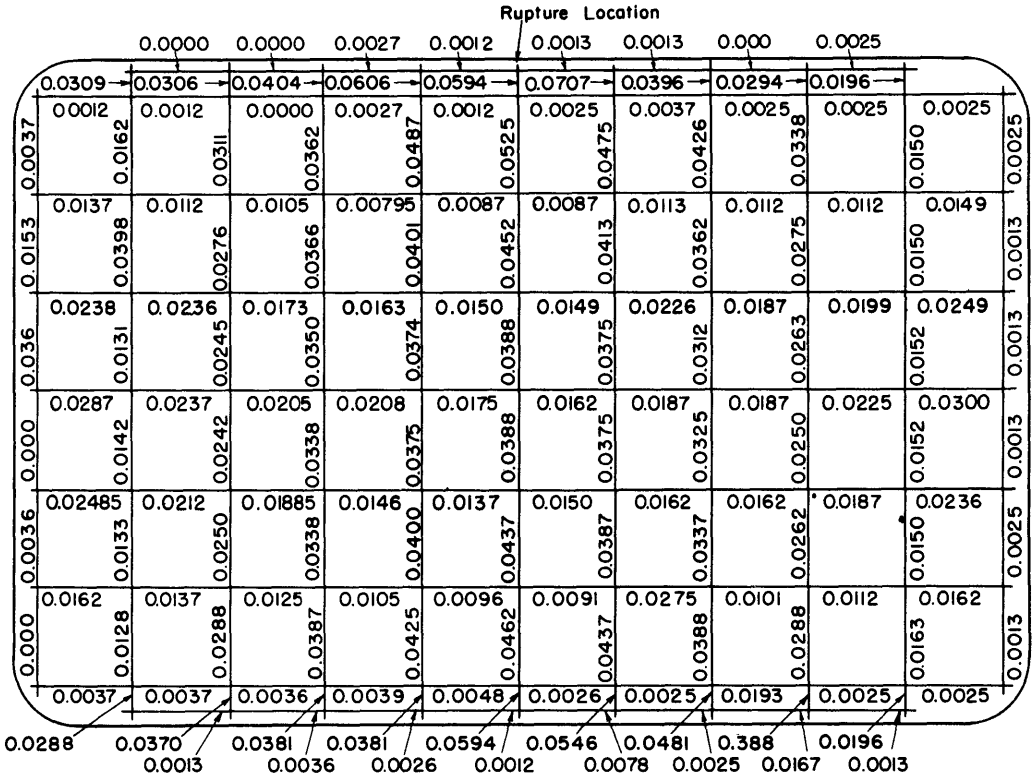

Figure 11a - Diaphragm 2A

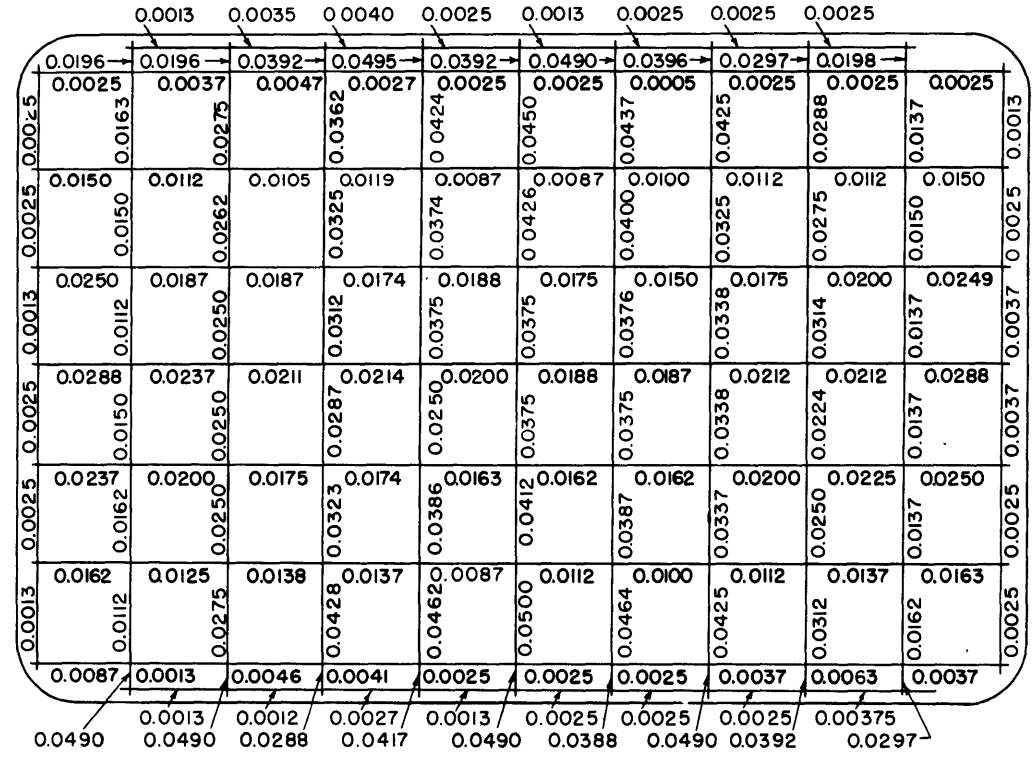

Figure 11b - Diaphragm 2B

Figure 11 - Final Plastic Strains in Inches per Inch

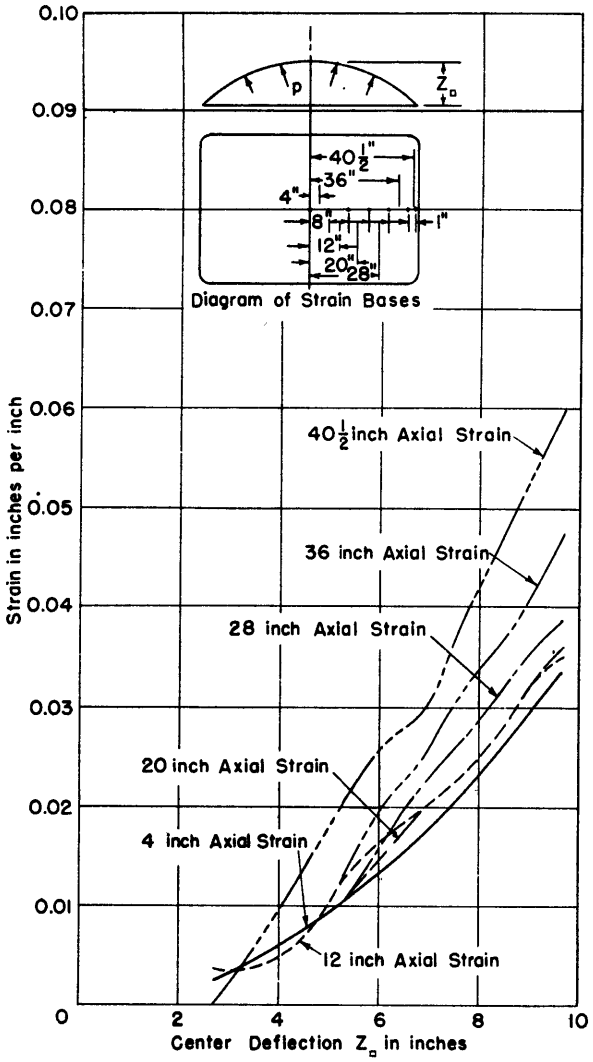

Figure 12a - Longitudinal

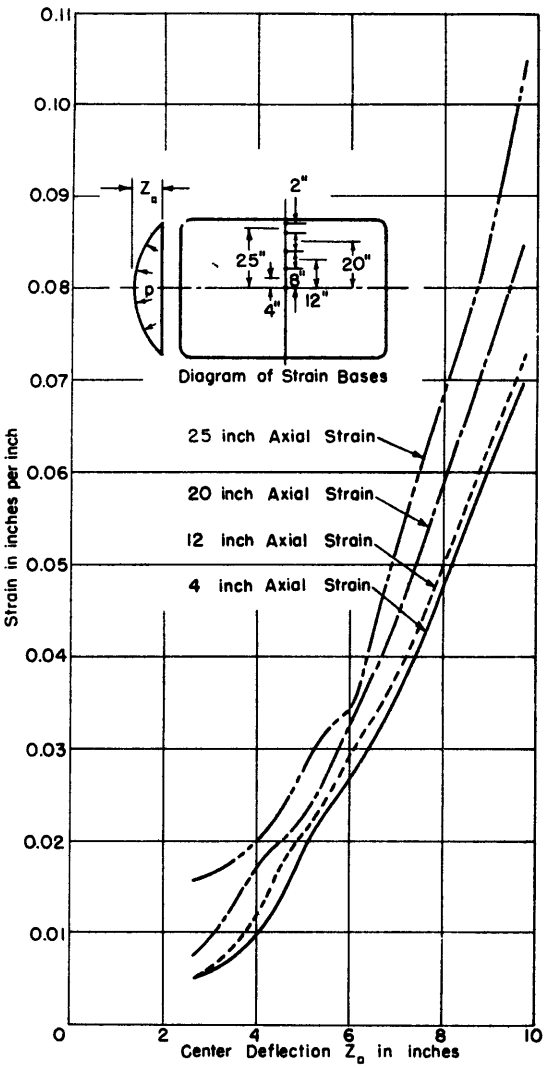

Figure 12b - Transverse

Figure 12 - Longitudinal and Transverse Axial Strains of 1/8-Inch Medium-Steel Diaphragm 1A

ENERGY ABSORBED BY DEFLECTED DIAPHRAGMS

Curves of energy absorption for the diaphragms appear in Figures 27 and 28. These curves were developed from pressure-volume curves constructed from test data. These energy data, along with the volume data mentioned in the previous paragraph, will be used later as a basis of comparison for theoretical methods of prediction of volume and energy absorption.

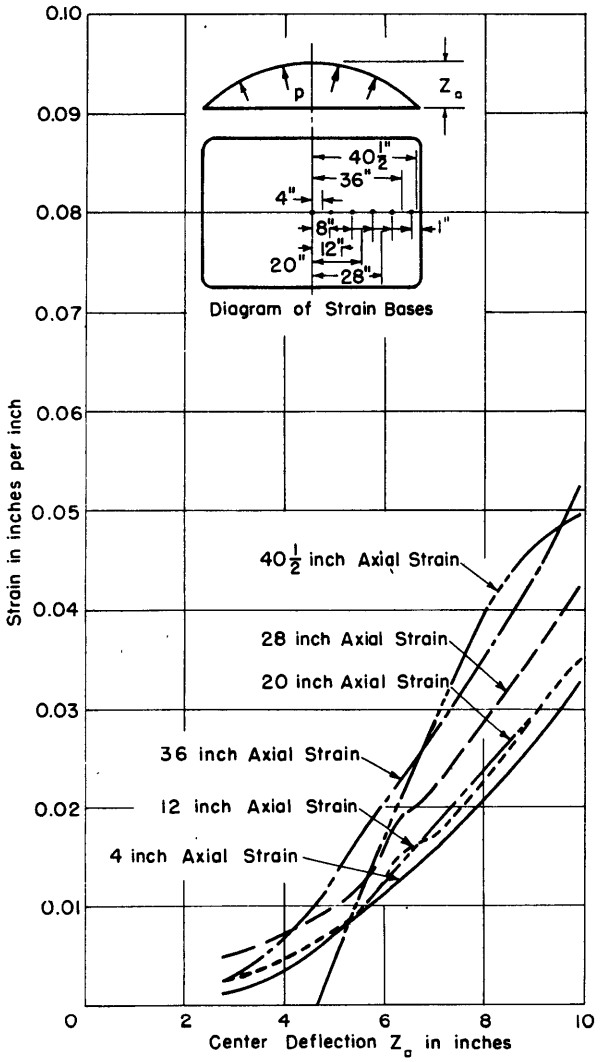

Figure 13a - Longitudinal

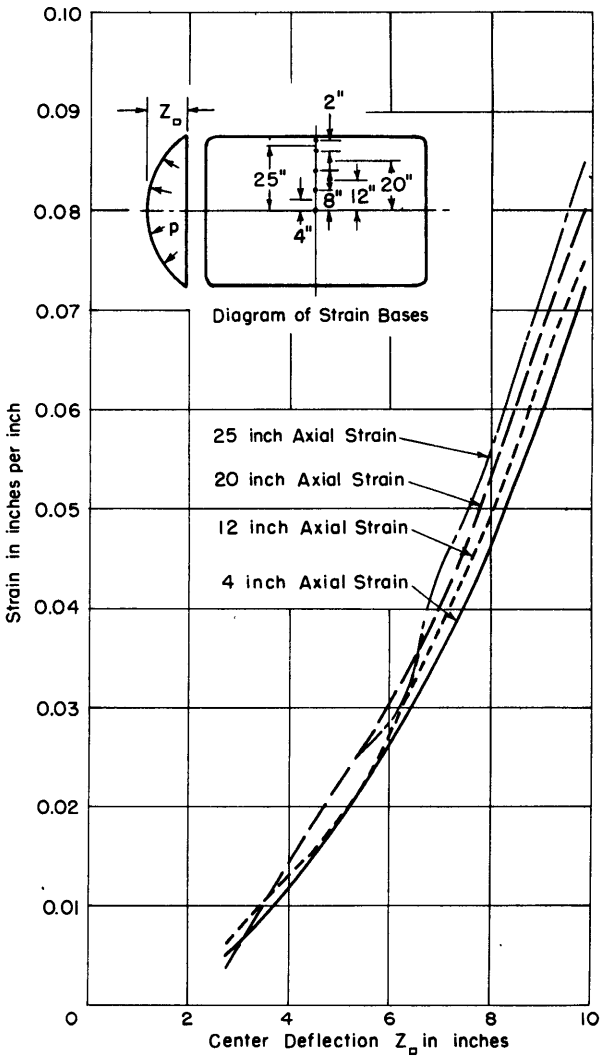

Figure 13b - Transverse

Figure 13 - Longitudinal and Transverse Axial Strains of 1/8-Inch Medium-Steel Diaphragm 1B

The approximate energy absorbed by a rectangular diaphragm for a given center deflection may be computed with the equation

$$W_{\square} = \frac{64}{45}\left(\frac{a_2}{a_1} + \frac{a_1}{a_2}\right)\sigma_{\square} h_{\square} Z_{\square}^2$$

Discussion of approximate energies occurs in a later section.

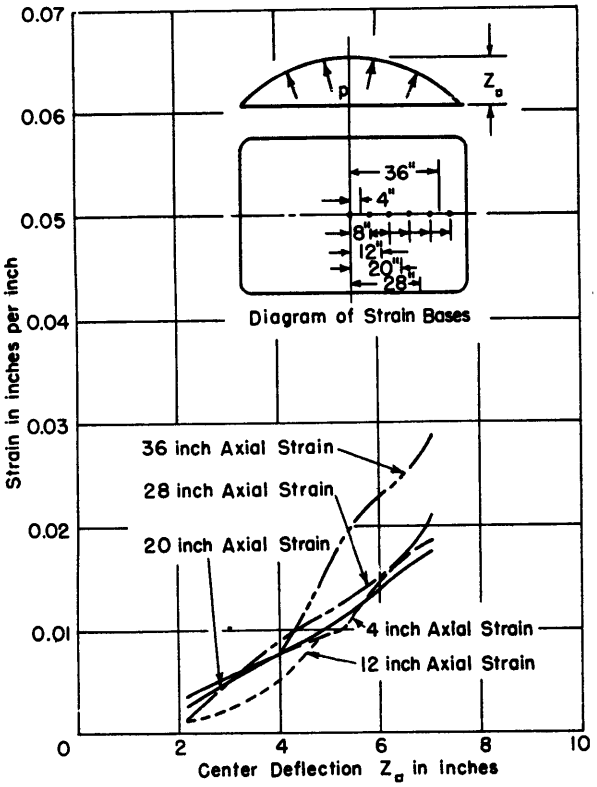

Figure 14a - Longitudinal

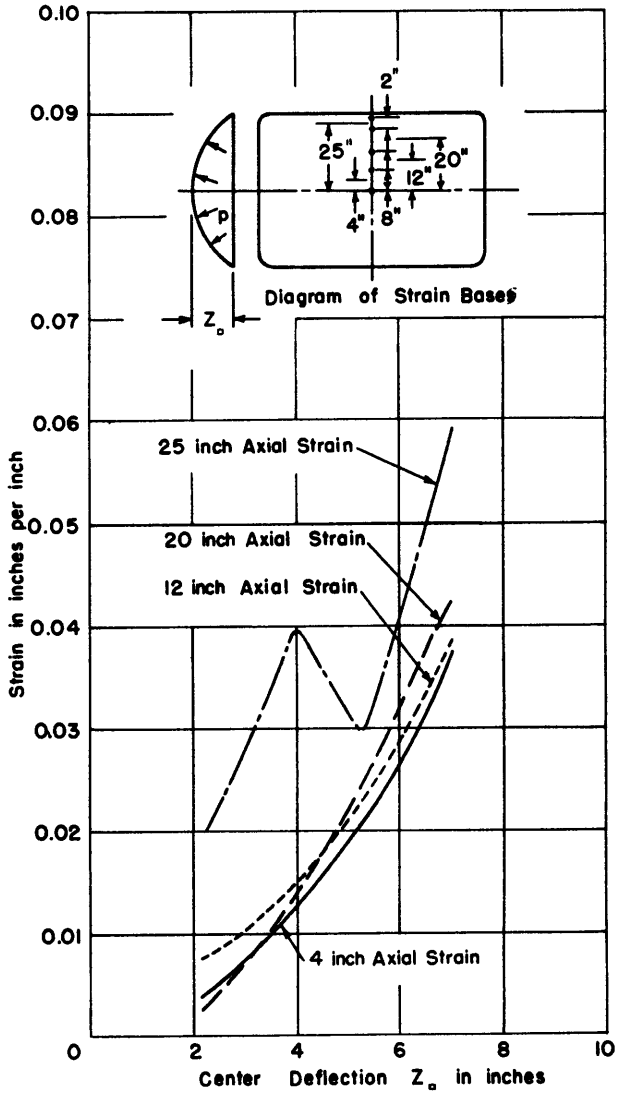

Figure 14b - Transverse

Figure 14 - Longitudinal and Transverse Axial Strains of 3/16-Inch Medium-Steel Diaphragm 2A

Figure 29 shows curves of the variance of approximate energy absorbed by a diaphragm. The values for the several curves were computed using selected values of unit stress $\sigma_{\square}$ as indicated in the figure. These stress values were obtained from the stress-strain diagrams of tensile coupon tests of the diaphragm material (Figure 30) and represent an average of the value taken from the curve parallel to the direction of rolling and the value transverse to the direction of rolling.

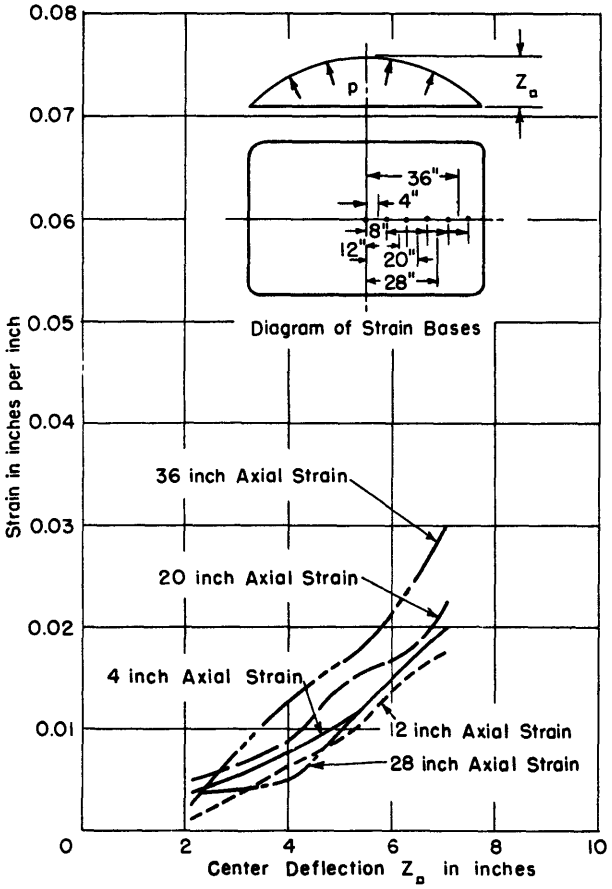

Figure 15a - Longitudinal

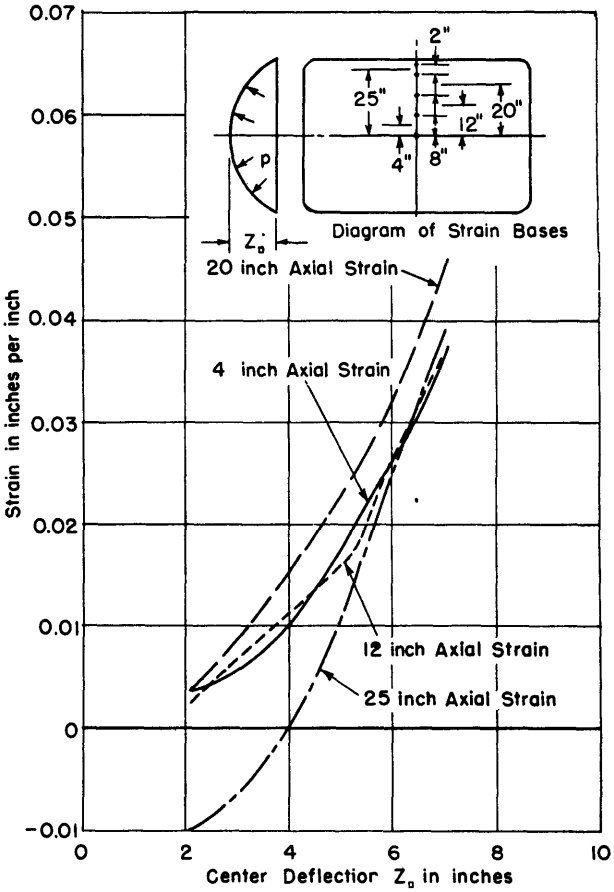

Figure 15b - Transverse

Figure 15 - Longitudinal and Transverse Axial Strains of 3/16-Inch Medium-Steel Diaphragm 2B

The energy-absorbing characteristics of diaphragms may be compared on a basis of the ratio of the "equivalent" radius to the diaphragm thickness, represented symbolically as $a_{\square}/h_{\square}$. The total energy absorbed per pound weight of a diaphragm, or unit energy absorbed, for a number of diaphragms might indicate an optimum value of this ratio and thus define the best geometry for a clamped diaphragm in point of energy absorption for a given kind of material. In the results of the small or pilot diaphragms (given in Table 2 of Reference 3), the unit energy values ranged from 360 foot-pounds to 1600 foot-pounds. The lowest value of energy represented a diaphragm with a ratio of 39, and the highest energy value a diaphragm with a ratio of 82. These diaphragms were of medium steel. A pair of diaphragms of furniture steel with an "equivalent" radius-thickness ratio of 93 and 91.5 showed a unit energy absorption of 1238 foot-pounds and 1138 foot-pounds, respectively. From Table 2 of this report the large diaphragms with ratios $a_{\square}/h_{\square}$ of 305 and 209 showed unit energies

(Text continued on page 25.)

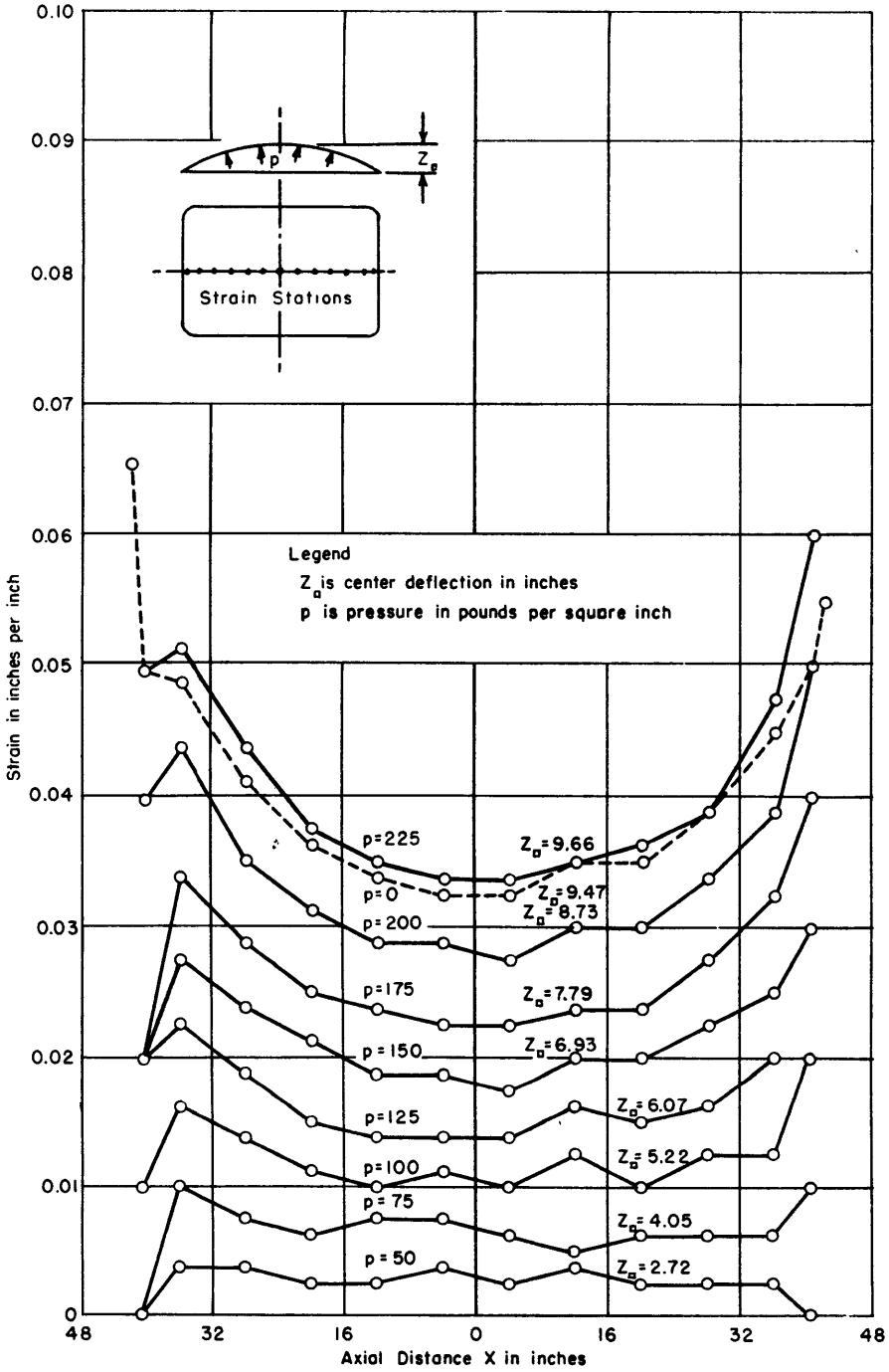

Figure 16a - Longitudinal

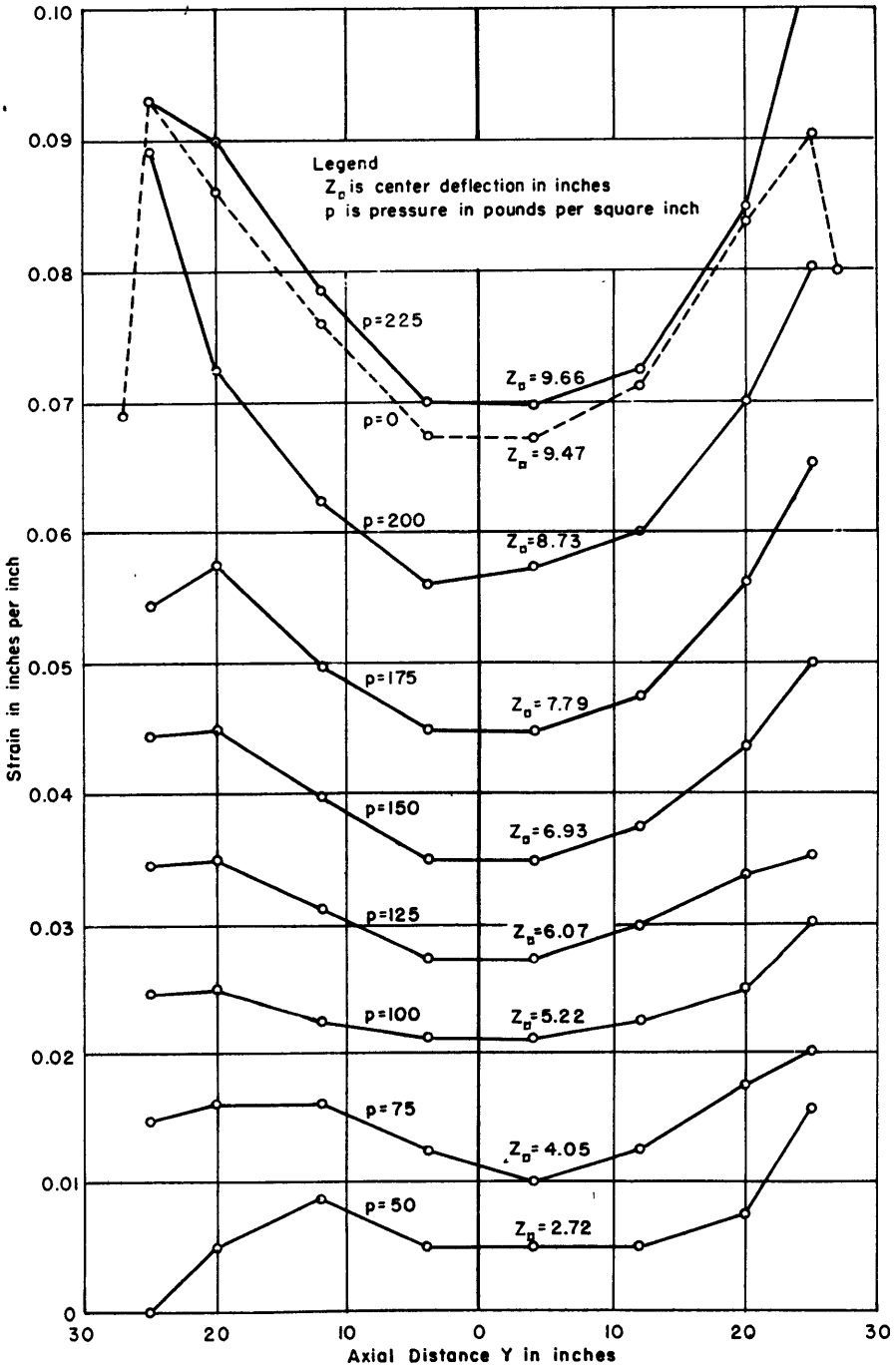

Figure 16b - Transverse

Figure 16 - Strain in 1/8-Inch Medium-Steel Diaphragm 1A Plotted against Axial Distance

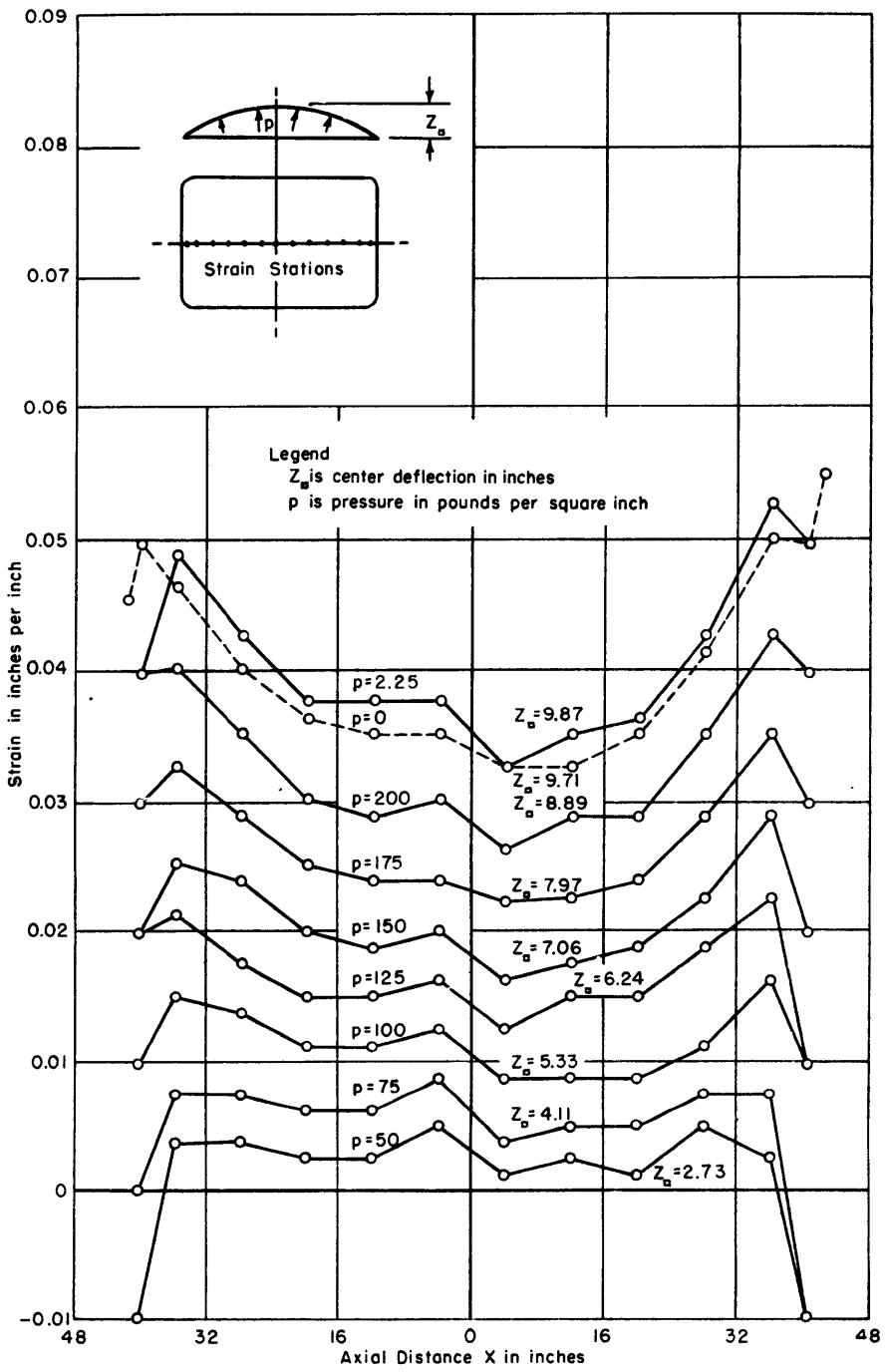

Figure 17a - Longitudinal

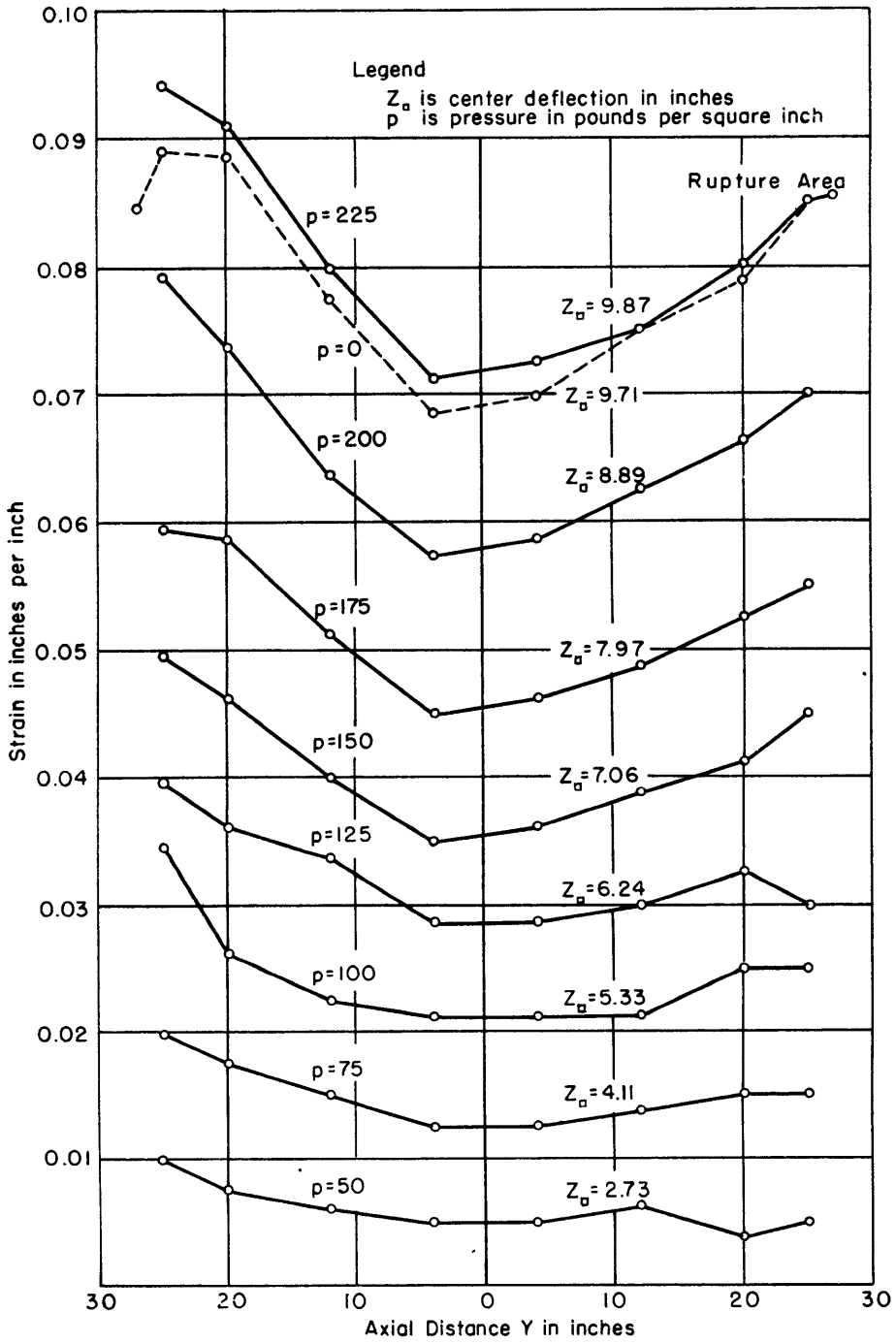

Figure 17b - Transverse

Figure 17 - Strain in 1/8-Inch Medium-Steel Diaphragm 1B Plotted against Axial Distance

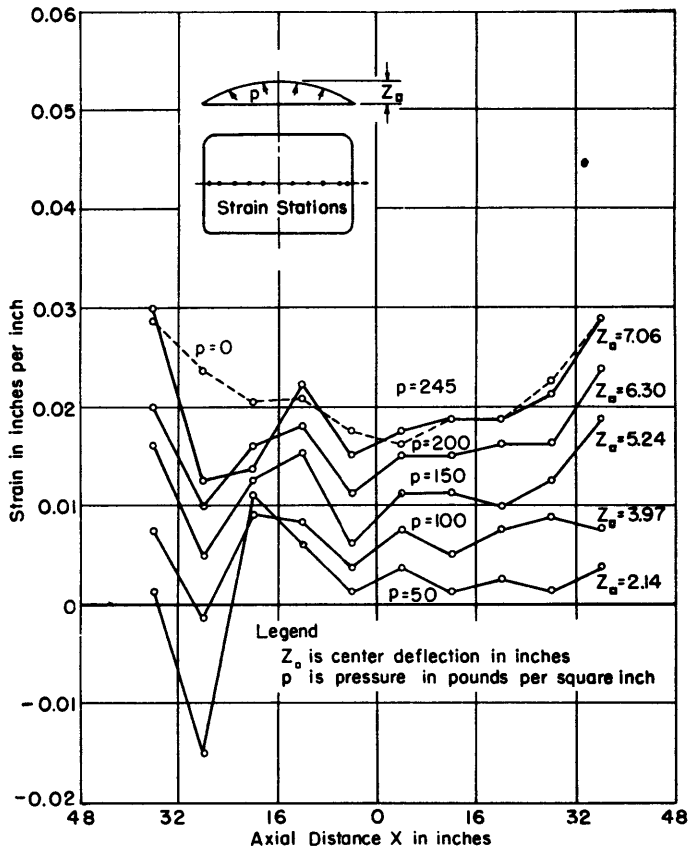

Figure 18a - Longitudinal

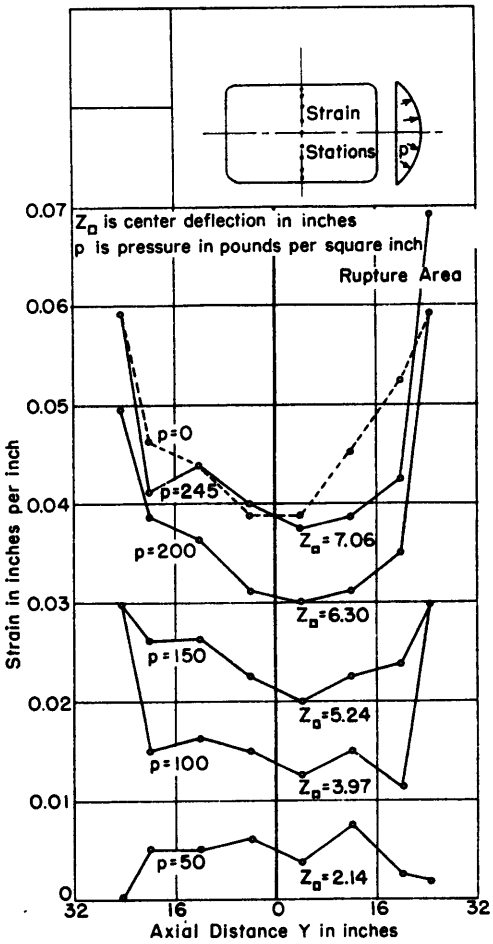

Figure 18b - Transverse

Figure 18 - Strain in 3/16-Inch Medium-Steel Diaphragm 2A Plotted against Axial Distance

absorbed of about 1200 foot-pounds and 600 foot-pounds, respectively. It would be difficult to draw any conclusion from these results that would hold for both the pilot and the large diaphragms. Where large differences in absolute area of diaphragms of similar material are involved, some sort of scale factor may be operative to change the optimum value of a_o/h_o.

COMPARISON OF EXPERIMENTAL RESULTS WITH THEORY

A theory which accounts for the behavior of thin, clamped, circular or rectangular diaphragms under increasing hydrostatic pressure was developed in Reference 5. The theory is based on two assumptions, one concerning the shape of thin, clamped, circular or rectangular diaphragms under hydrostatic pressure, and the other concerning the invariance of energy absorption as a

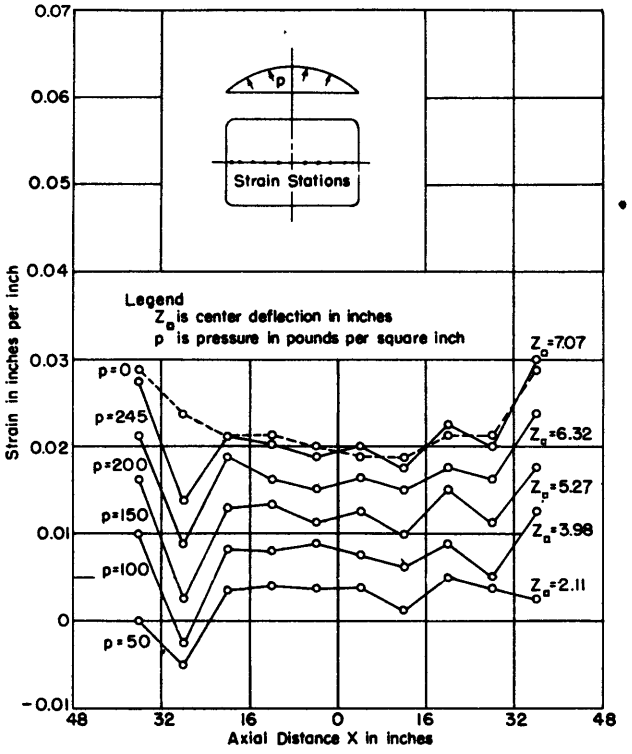

Figure 19a - Longitudinal

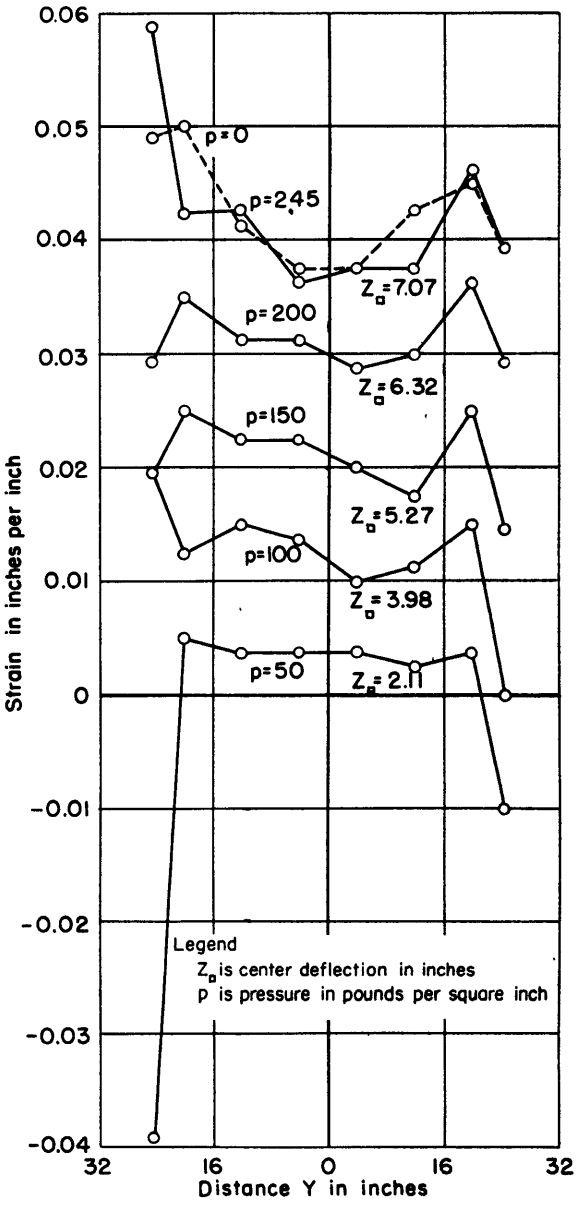

Figure 19b - Transverse

Figure 19 - Strain in 3/16-Inch Medium-Steel Diaphragm 2B
Plotted against Axial Distance

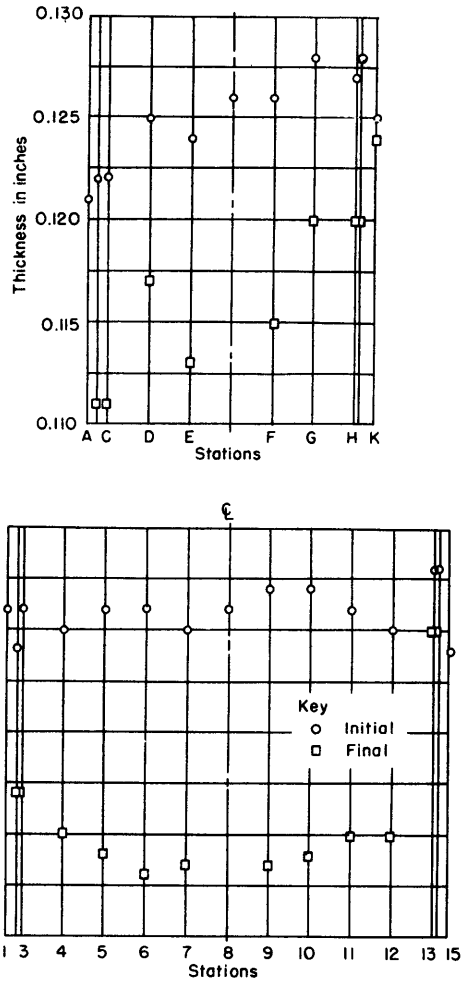

Figure 20 - Initial and Final Thicknesses of Diaphragm 1A

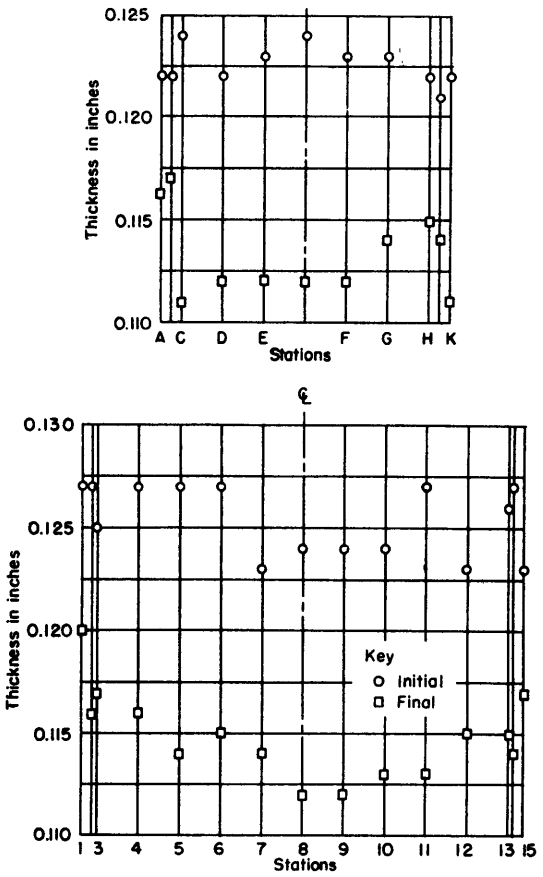

Figure 21 - Initial and Final Thicknesses of Diaphragm 1B

function of the areal strain of thin diaphragms. The tension, or force per unit length, in a biaxially stressed diaphragm is approximately constant because of the balancing of the strain-hardening of the material with the reduction in thickness as the stress increases. The relation between the center deflections of two diaphragms of like material and the pressures which produce these deflections is expressed by simple algebraic equations involving the physical dimensions of the diaphragms. Thus, if the pressure-deflection function of a diaphragm is known, the diaphragm may be used as a model or "equivalent" diaphragm by which the theory may be applied for the prediction of pressure and center deflection for any other circular or rectangular diaphragm of the same material. By use of measured values of ultimate stress obtained from a standard tensile test, the equations can be extended to diaphragms of different materials. The energy absorbed in the plastic deflection of any circular or rectangular diaphragm may also be predicted.

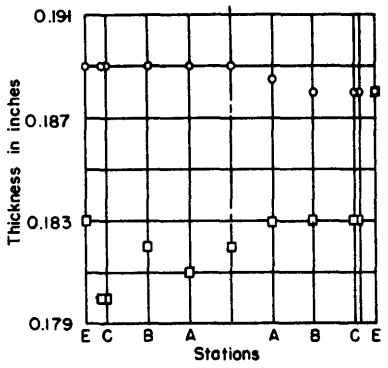

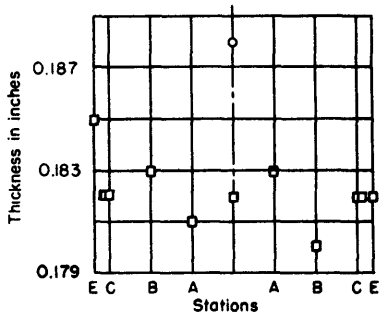

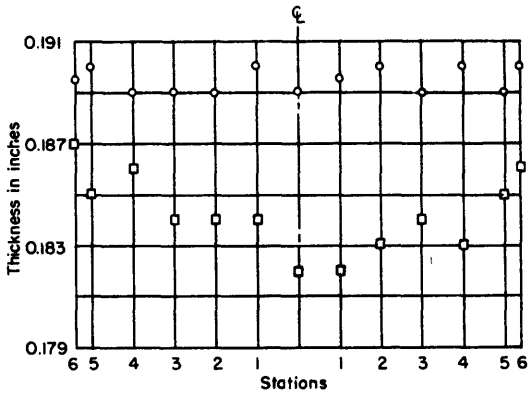

Figure 22 - Initial and Final Thicknesses of Diaphragm 2A

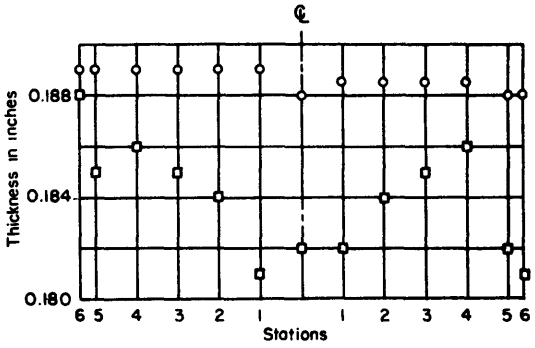

Figure 23 - Initial and Final Thicknesses of Diaphragm 2B

In the following sections results predicted by this theory are compared with experimental results obtained in the present tests on rectangular diaphragms.

THE VOLUME EQUATION

Gleyzal[5] has developed an equation for the volume displaced by a diaphragm as it deflects under hydrostatic pressure, based on the assumption that the diaphragms deflect parabolically. The actual measured final volumes for the four diaphragms of the present test are compared with the volumes computed by Gleyzal's volume equation for a rectangular diaphragm, namely,

$$V = \frac{16}{9} a_1 a_2 Z_\square$$

where a_1 and a_2 are the semi-length and semi-width of the diaphragm and $Z_\square$ is the center deflection. Table 2 shows the final measured volumes and the computed volumes and the percentage of variance of the computed volumes from the

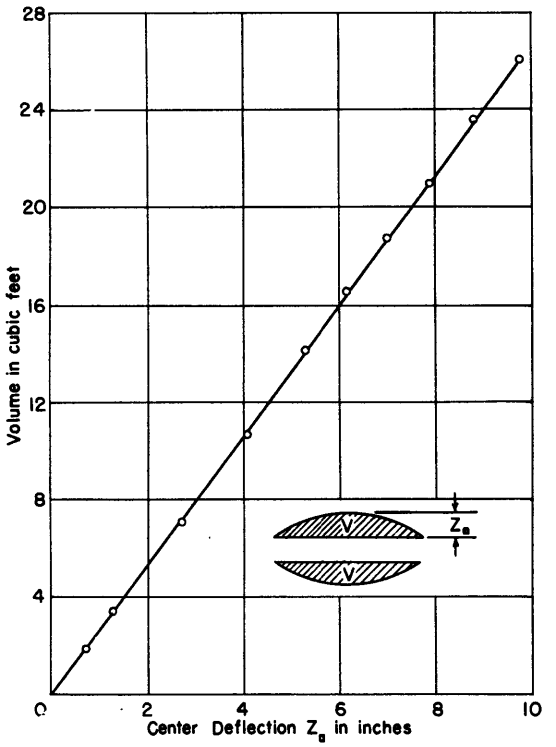

Figure 24 - Volume Change of 1/8-Inch Diaphragms 1A and 1B Plotted against Center Deflection

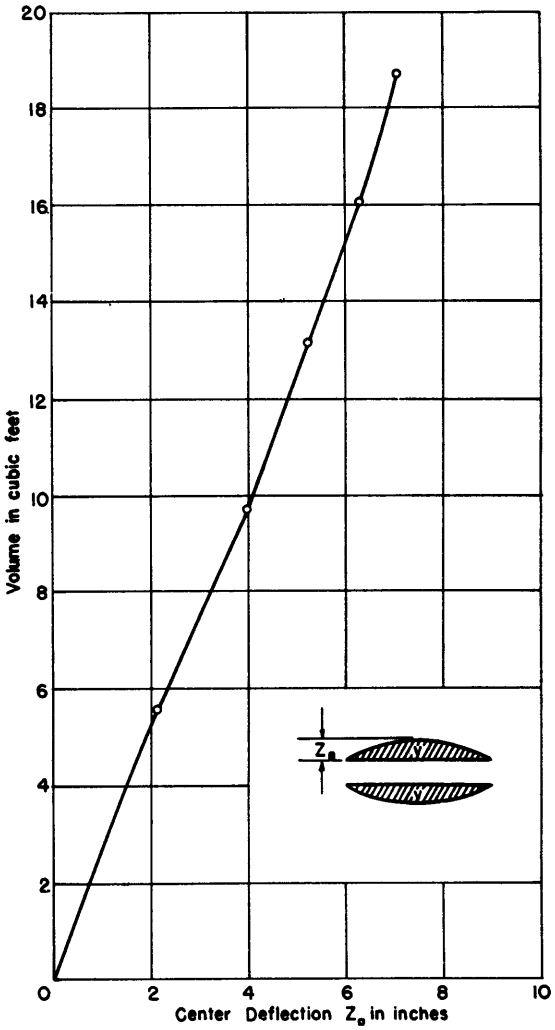

Figure 25 - Volume Change of 3/16-Inch Diaphragms 2A and 2B Plotted against Center Deflection

measured volumes. Figure 26 shows curves for volume variance for two diaphragms for the complete range of test pressures. These data indicate that the volume equation is accurate to within -12 percent.

EQUIVALENT RADIUS: THE FUNCTION ϕ

According to Reference 5 two diaphragms are in corresponding states if their areal strains are equal. One diaphragm may be circular, and one may be rectangular. This relation is expressed in the equation

$$\frac{Z_o^2}{a_o^2} = \frac{16}{45} Z_\square^2 \left(\frac{1}{a_1^2} + \frac{1}{a_2^2} \right)$$

where Z_o is the center deflection of the circular diaphragm in inches,
a_o is the radius of the circular diaphragm in inches,
$Z_\square$ is the center deflection of the rectangular diaphragm in inches,
a_1 is the semi-major axis of the rectangular diaphragm in inches, and
a_2 is the semi-minor axis of the rectangular diaphragm in inches.

The rectangular and circular subscripts refer to rectangular and circular diaphragms respectively. The above equation suggests a definition for equivalent radius $a_\square$ of a rectangular diaphragm which can be expressed as

$$\frac{1}{a_\square^2} = \frac{16}{45}\left(\frac{1}{a_1^2} + \frac{1}{a_2^2} \right) \text{ or } a_\square = \frac{a_1 a_2}{4} \sqrt{\frac{45}{a_1^2 + a_2^2}}$$

The appropriate relations for center deflection, energy absorption, and pressure may be stated from Reference 5 to be as follows:

If

$$\frac{Z}{a} = \frac{Z_\square}{a_\square} = \frac{Z_o}{a_o}$$

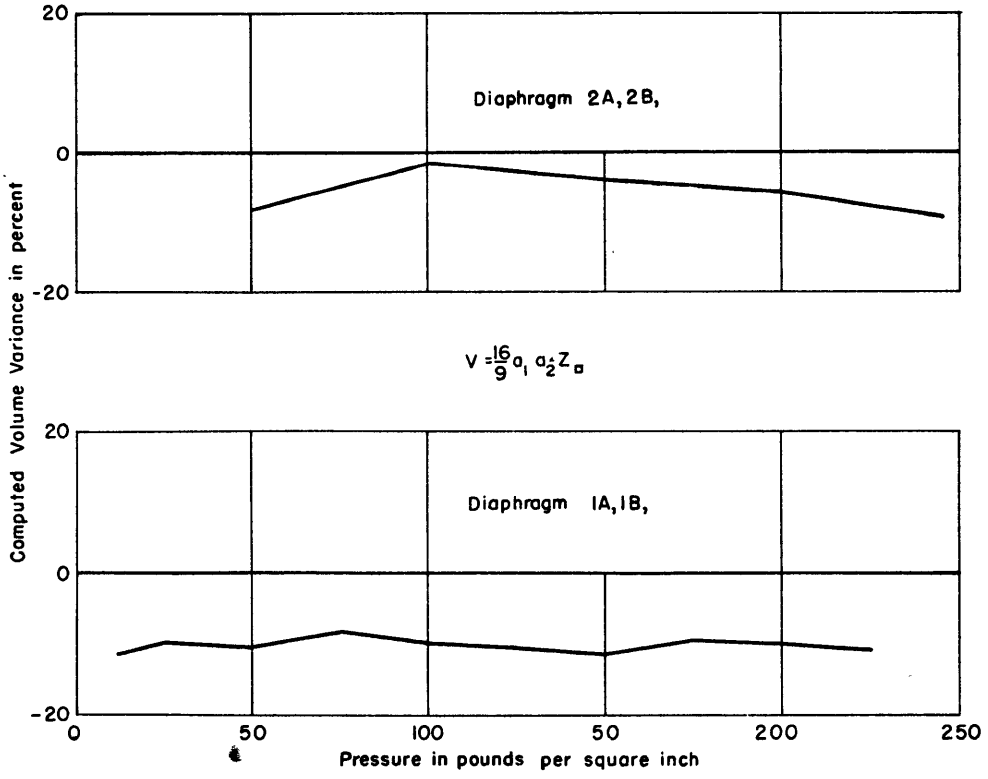

Figure 26 - Variance of Computed Volume from Actual Measured Volume

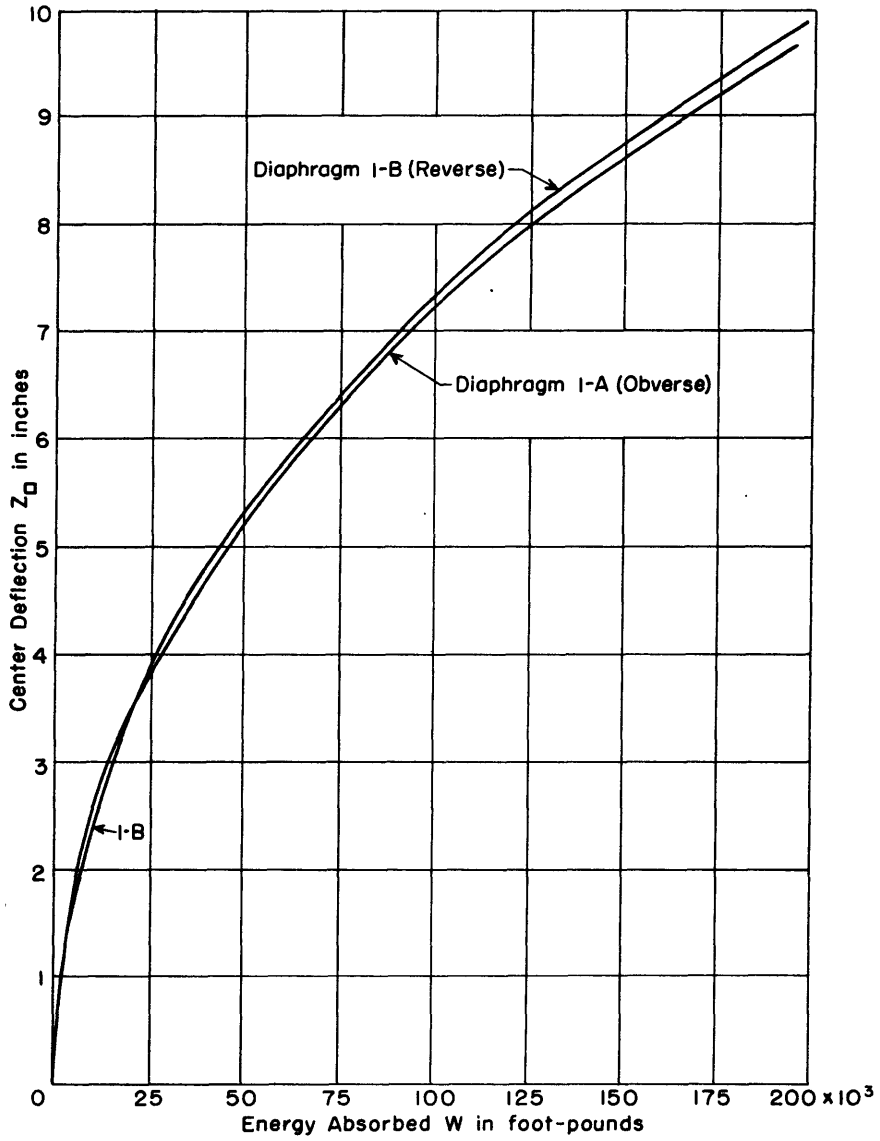

Figure 27 - Curves of Energy Absorption Plotted against Center Deflection for 1/8-Inch Diaphragms 1A and 1B

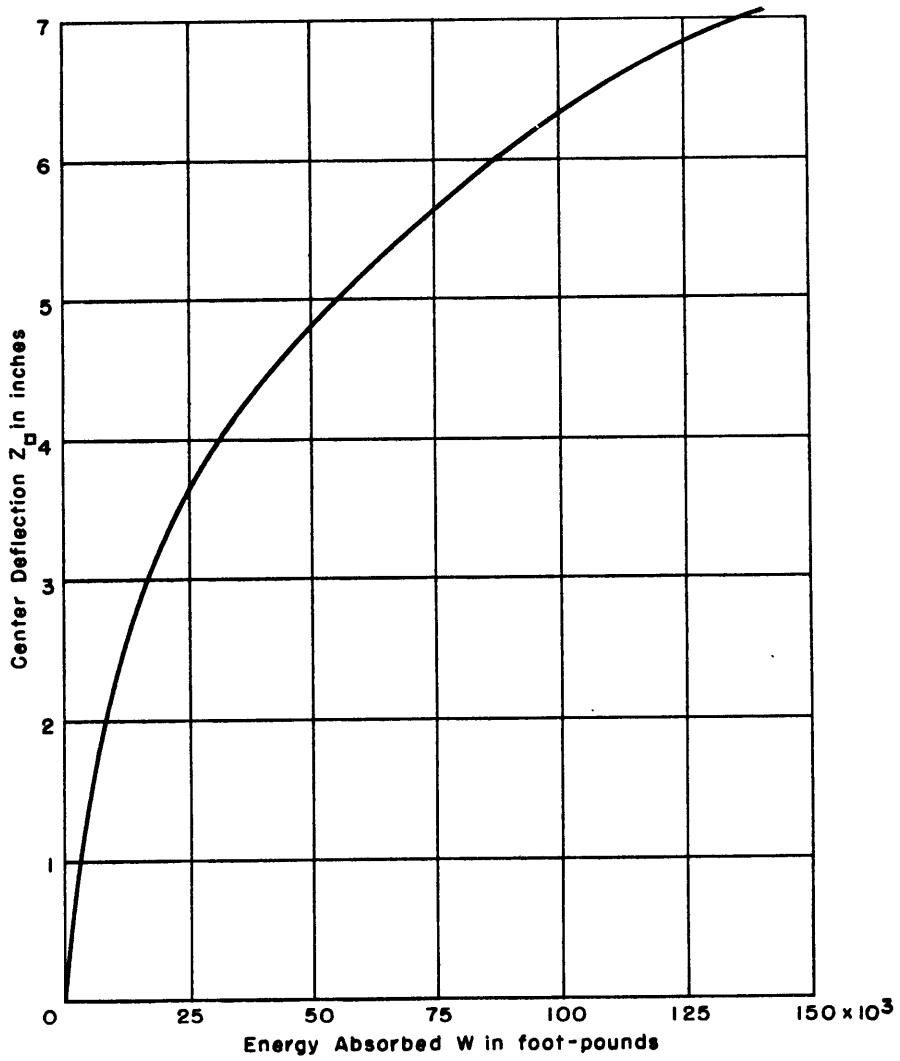

Figure 28 - Curves of Energy Absorption Plotted against Center Deflection for 3/16-Inch Diaphragms 2A and 2B

In the range tested, the energy curves for diaphragms 2A and 2B coincided.

then

$$\frac{W}{\bar{W}} = \frac{W_\square}{4\, a_1 a_2 \sigma_\square h_\square} = \frac{W_o}{\pi a_o^2 \sigma_o h_o} = \phi\left(\frac{Z}{a}\right)$$

and

$$\frac{1}{2} P = \frac{4}{9} \frac{p_\square a_\square}{\sigma_\square h_\square} = \frac{1}{2} \frac{p_o a_o}{\sigma_o h_o} = \phi'\left(\frac{Z}{a}\right)$$

where W. $W_\square$, or W_o is the energy absorbed by a diaphragm under increasing pressure in inch-pounds,

$\bar{W}$ is equal to $4\sigma_\square h\, a_1 a_2$ or $\sigma_o h \pi a_o^2$,

$a_\square$ is the equivalent radius of the rectangular diaphragm in inches,

$h_\square$ or h_o is the original thickness of the diaphragm in inches,

p is the applied hydrostatic pressure in pounds per square inch,

$\sigma_\square$ or σ_o is a stress representing the strength of the diaphragm material measured in the same way for both diaphragms, e.g., it may be the "ultimate" stress, and

P and $\frac{Z}{a}$ are quantities defined by the equations.

The rectangular and circular subscripts refer to rectangular and circular diaphragms respectively, and ϕ is the same function for all thin, clamped, rectangular or circular diaphragms.

As explained in Reference 3, the function $\phi\left(\frac{Z}{a}\right)$ may be determined from observations on a diaphragm and may then be used to predict the energy absorption for any rectangular or circular diaphragm. In Figure 31 is shown a curve representing ϕ, based on the results for the four rectangular diaphragms tested; the plotted points represent values of $W/\overline{W}$ and $Z_\square/a_\square$ computed from each pressure stage of each of the diaphragms. Figure 31 agrees reasonably well with Figure 21 of Reference 3.

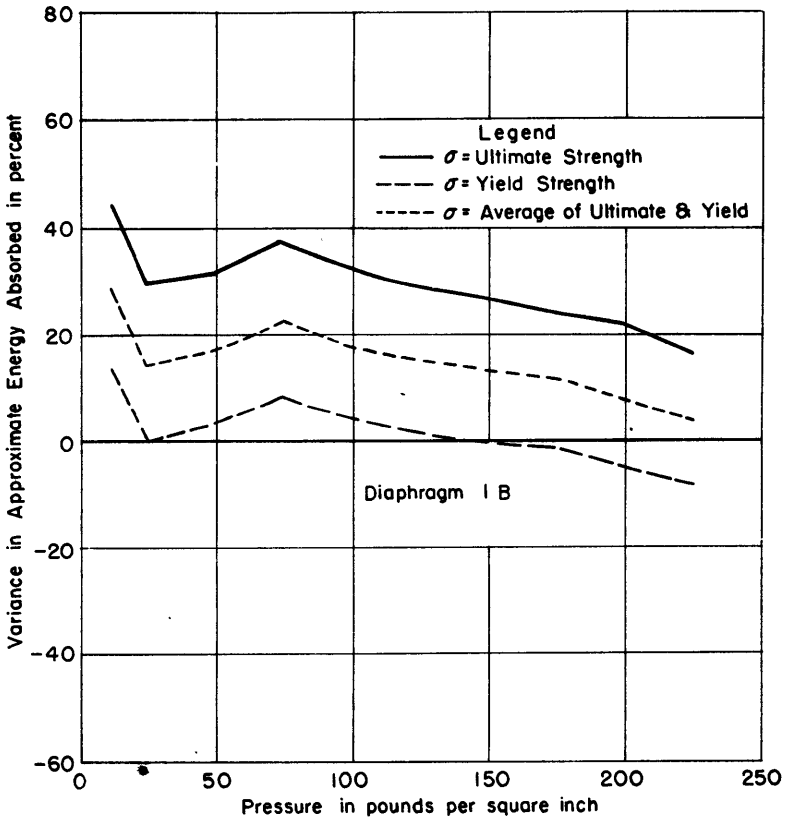

Figure 29 - Variance of Approximate Energy from Measured Energy Absorbed

$$W = \frac{64}{45}\left(\frac{a_2}{a_1} + \frac{a_1}{a_2}\right)\sigma_\square h_\square Z_\square^2$$

EXPERIMENTAL AND THEORETICAL PRESSURE-DEFLECTION CURVES

Figure 32 of this report and Figure 22 of Reference 3 and Figure 3 of Reference 5 display experimental pressure-deflection curves for all unstiffened circular and rectangular diaphragms discussed in this report and in Reference 3. All these data are directly comparable as each of the three figures are set up on identical coordinate systems. The experimental curves for the large diaphragms of the present test fall well within the limits of those for the small diaphragms.

Figure 32 includes also a curve obtained by exact membrane theory for a rectangular diaphragm whose aspect ratio is 3/2. This curve was obtained by the following procedure. A convenient value for $Z_\square/a_\square$ was assumed, the "equivalent radius" of the rectangular diaphragm $a_\square$ was known, and the corresponding value of the center deflection $Z_\square$ was obtained. The "equivalent pressure" P was determined by use of Equations [19] and [22] of Reference 5. The right-hand member of Equation [22],

$$p_\square = 4.84 \frac{\sigma_\square h_\square Z_\square}{a_\square^2}$$

was substituted for $p_\square$ in Equation [19],

$$P = \frac{8}{9} \frac{p_\square a_\square}{\sigma_\square h_\square}$$

and this operation produced the expression

$$P = 4.3 \frac{Z_\square}{a_\square}$$

from which the quantity P was computed. The values for P thus obtained were plotted against the value for $Z_\square/a_\square$ to construct the curve.

The curve obtained from exact membrane theory for a circular diaphragm may be similarly obtained by use of the right-hand member of the equation

$$p_o = 4 \frac{\sigma_o h_o Z_o}{a_o^2 + Z_o^2}$$

from Reference 5, page 13, in substitution for p_o in Equation [19], Reference 5,

$$P = \frac{p_o a_o}{\sigma_o h_o}$$

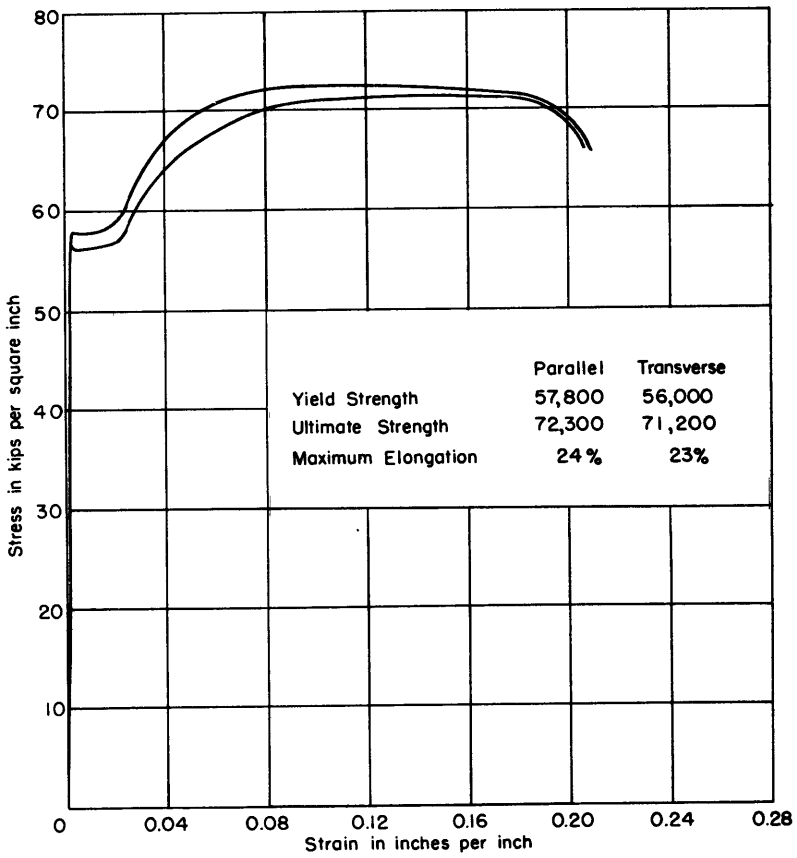

Figure 30a - Diaphragms 1A and 1B

This operation produces the expression for "equivalent pressure"

$$P = 4\frac{a_o Z_o}{a_o^2+Z_o^2}$$

The "equivalent pressure" may also be determined by the equation (Reference 5, page 12)

$$P = 4\frac{\frac{Z_o}{a_o}}{1+\frac{Z_o^2}{a_o^2}}$$

The values of P obtained by either of the above methods may then be plotted against the chosen value of Z_o/a_o, and the graph for exact membrane theory for circular diaphragms drawn as shown in Figure 32.

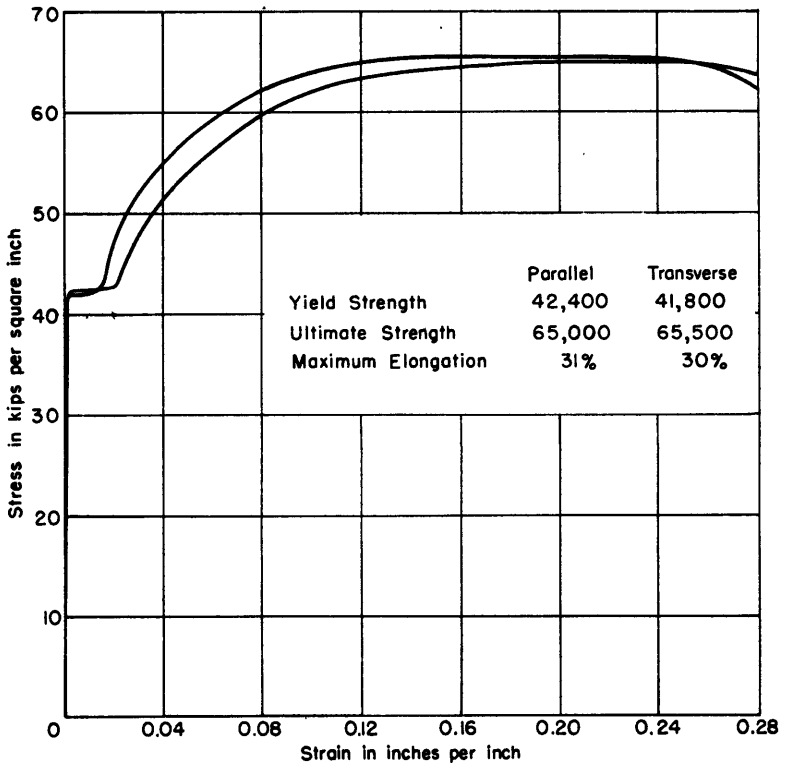

Figure 30b - Diaphragms 2A and 2B

Figure 30 - Tensile Stress-Strain Curve for Medium Steel Diaphragms 1A, 1B, 2A and 2B

One specimen was cut with its long dimension parallel to the direction of rolling, the other transverse to the direction of rolling.

APPROXIMATE EQUATION FOR ENERGY ABSORBED

The approximate expression for the energy absorbed by a thin rectangular diaphragm as developed in Reference 5 takes the form:

$$W_{\square} = \frac{64}{45}\left(\frac{a_2}{a_1} + \frac{a_1}{a_2}\right)\sigma_{\square} h_{\square} Z_{\square}^2$$

where a_1 and a_2 are the semi-length and semi-width of the diaphragm in inches,

$\sigma_{\square}$ is a stress representing the strength of the diaphragm material measured in the same way for any material, e.g., it may be the "ultimate" stress,

$h_{\square}$ is the initial thickness of the diaphragm in inches, and

$Z_{\square}$ is the center deflection of the diaphragm in inches.

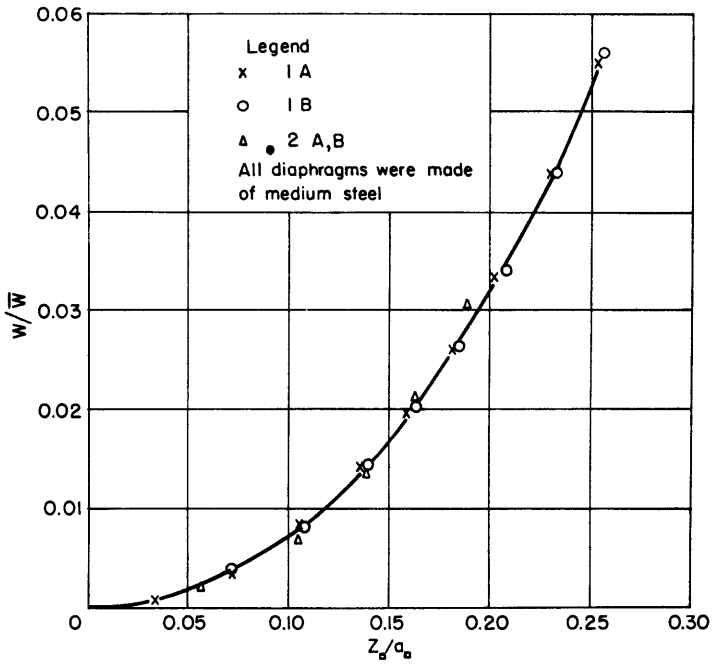

Figure 31 - Curve for the Function ϕ as Expressed by the Relation

$$\frac{W}{\bar{W}} = \phi \frac{Z_{\square}}{a_{\square}}$$

The approximate values of energy and the variance of these values from experimental values are given in Table 2 for the final deflection conditions of the diaphragms. The variance values show considerable spread among the several diaphragms. By reason of this condition it was decided to explore the variances for pressures over the range of a diaphragm test. Figure 29 shows plots of variance of approximate energy absorbed from measured energy for the complete range of tests of Diaphragm 1B, using for $\sigma_{\square}$ the ultimate strength of the diaphragm material. Plots using yield strength and the average of yield and ultimate strengths are also shown. These two additional plots represent attempts to find a value for $\sigma_{\square}$ that would make a useful tool of the equation for prediction of the approximate energy. Using the yield strength of the material as a value of $\sigma_{\square}$, the approximate equation for energy may be considered to be reliable within ± 15 percent.

The low accuracy of the approximate equation for energy absorbed may be due to the possibility that a rectangular diaphragm, because of its shape, acts less like a membrane than does a circular diaphragm. In the circular diaphragm the strain-hardening effects tend to balance the effects of decrease in thickness of the diaphragm as the pressure increases, thus making the tension in the material more or less constant.

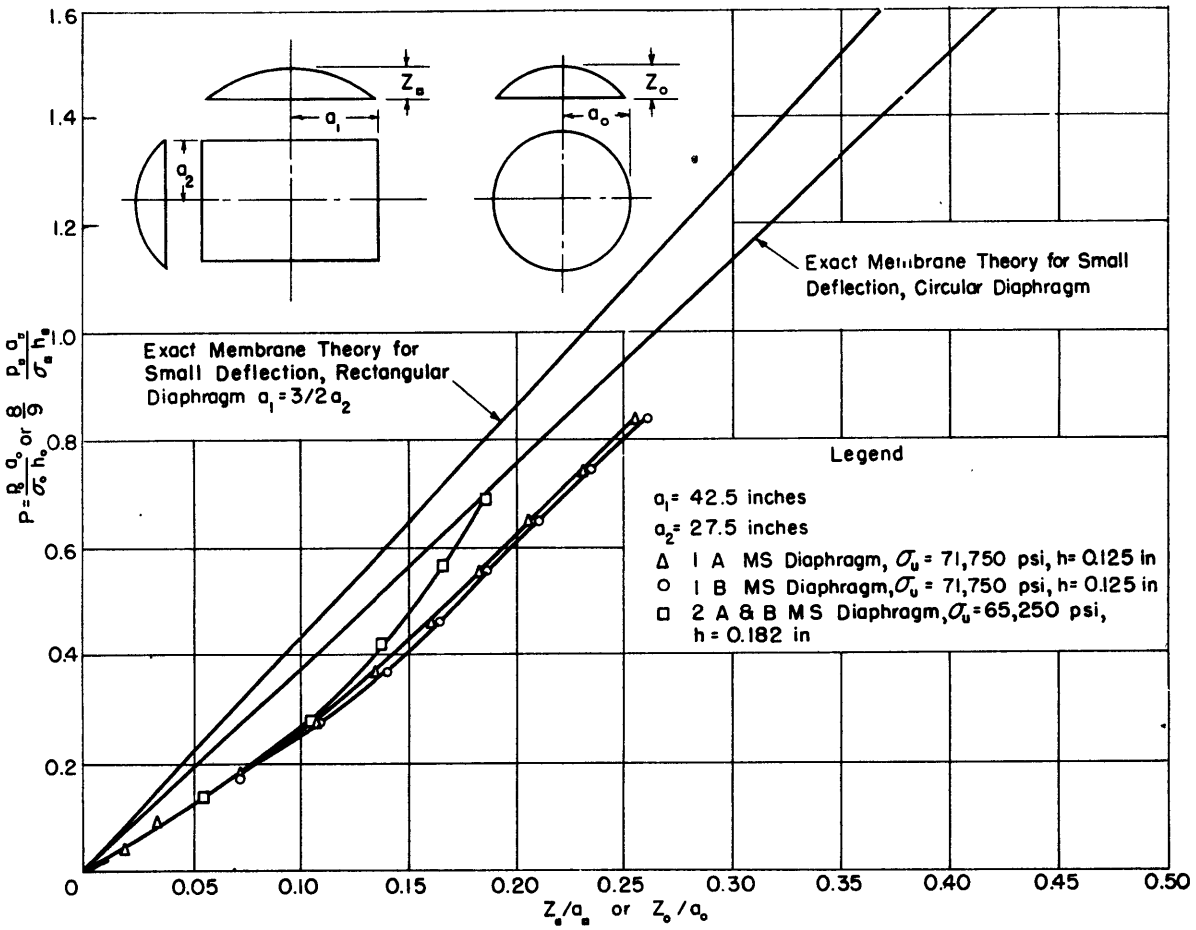

Figure 32 - Experimental and Theoretical Curves Showing Relation between Pressure and Center Deflection for Thin Circular and Rectangular Diaphragms

CONCLUSIONS

1. The testing techniques used in the present tests, which were developed during similar tests on smaller diaphragms, were successful.

2. The equation for computing the volume displaced by a dished rectangular diaphragm with clamped edges is accurate to -15 percent.

3. The equation for approximate energy absorbed by a diaphragm deformed by hydrostatic pressure was reliable only to $\pm$ 15 percent, using the yield stress from a tensile test as a value of σ. The low accuracy of the equation may be due to the possibility that a rectangular diaphragm acts less like a membrane than does a circular diaphragm.

Since the theory is comparative and not absolute, a choice of the stress value may be exercised. In the pilot and the present tests a system using σ equivalent to tensile yield stress up to 65 percent of expected center deflection, and use of tensile ultimate stress for the remainder of the deflection range, proved moderately satisfactory for predicting energies. Using this system the equation may be concluded to be reliable to +20 percent.

4. In the expression $\frac{W}{\bar{W}} = \phi \frac{Z}{a}$ experimental determination of ϕ was made and the statement in the original theory that if the function ϕ is determined experimentally for one clamped thin diaphragm it is the same for all other clamped thin diaphragms was proved. The locus of the function ϕ was essentially the same for all diaphragms tested.

REFERENCES

1. TMB CONFIDENTIAL ltr C-S81-3 of 9 September 1943 to Chief of the Bureau of Ships, Ship Protection (374).

2. BuShips CONFIDENTIAL ltr C-S81-3(374) of 16 September 1943 to TMB.

3. Day, J.W., "Hydrostatic Tests on Thin Rectangular Diaphragms 21 Inches by 13 1/2 Inches," TMB Report 635, March 1951.

4. Gleyzal, A.N., Ph.D., "Plastic Strain and Deflection Tests on Clamped Circular Steel Plates 20 Inches in Diameter," TMB Report R-142, May 1944.

5. Gleyzal, A.N., Ph D., "Plastic Deformation and Energy Absorption of a Thin Rectangular Plate under Hydrostatic Pressure," TMB Report R-280, January 1945.